Reducing the Flexibility of Type II Dehydroquinase for Inhibition: A Fragment-Based Approach and Molecular Dynamics Study

Antonio Peón,[a] Adrián Robles,[a] Beatriz Blanco,[a] Marino Convertino,[b, d] Paul Thompson,[c] Alastair R. Hawkins,[c] Amedeo Caflisch,*[b] and Concepción González-Bello*[a]

A multidisciplinary approach was used to identify and optimize a quinazolinedione-based ligand that would decrease the flexibility of the substrate-covering loop (catalytic loop) of the type II dehydroquinase from *Helicobacter pylori*. This enzyme, which is essential for the survival of this bacterium, is involved in the biosynthesis of aromatic amino acids. A computer-aided fragment-based protocol (ALTA) was first used to identify the aromatic fragments able to block the interface pocket that separates two neighboring enzyme subunits and is located at the active site entrance. Chemical modification of its non-aro-matic moiety through an olefin cross-metathesis and Seebach's self-reproduction of chirality synthetic principle allowed the development of a quinazolinedione derivative that disables the catalytic loop plasticity, which is essential for the enzyme's catalytic cycle. Molecular dynamics simulations revealed that the ligand would force the catalytic loop into an inappropriate arrangement for catalysis by strong interactions with the catalytic tyrosine and by expelling the essential arginine out of the active site.

Introduction

Although antibiotics are one of the most successful drugs in the clinic that have saved millions of lives, many of them are nowadays ineffective in treating infections caused by resistant bacteria.[1] This is a significant problem in people with weakened immune systems or who are undergoing surgery, cancer chemotherapy, dialysis, etc., for which the treatment of secondary processes are crucial. One of the factors responsible for the current resistance levels is the fact that most of the antibiotics in clinical use target the same types of bacterial targets, and resistance to them are well known and spread worldwide. To this end, in recent years much research has been devoted to the identification of new and unexploited therapeutic targets involved in key processes for bacterial survival as well as the detailed insight of the basis of their behavior and the identification of compounds targeting them.

One of these interesting targets is the type II dehydroquinase (3-dehydroquinate dehydratase, DHQ2, EC 4.2.1.10) that is the third enzyme of the shikimic acid pathway, through which erythrose-4-phosphate and phosphoenol pyruvate is converted into chorismic acid. The latter is the precursor of important aromatic metabolites such as the aromatic amino acids, folate cofactors, ubiquinone and vitamins E and K.[2] DHQ2, which is encoded by the *aroD/aroQ* gene, is an essential enzyme in *Mycobacterium tuberculosis*, the causative agent for tuberculosis, and *Helicobacter pylori*, which is a major cause of gastric and duodenal ulcers and it has been classified as class I carcinogen by the International Agency of Research on Cancer (IARC) and World Health Organization (WHO).[3, 4]

DHQ2 catalyzes the reversible dehydration of 3-dehydroquinic acid (**1**) to form 3-dehydroshikimic acid (**3**) via the enolate intermediate **2** (Figure 1).[5, 6] Extensive biochemical, structural and quantum mechanics/molecular mechanics (QM/MM) studies revealed that the enzymatic reaction is initiated by an essential aspartate that deprotonates an essential tyrosine to afford the catalytic tyrosinate, which triggers the process.[5–7] The necessary decrease in pK_a of the tyrosine is achieved by the proximity of two conserved arginine residues and a cation–π interaction with an essential arginine. The final step is the acid-catalyzed elimination of the C1 hydroxy group that is mediated by the conserved histidine acting as a proton donor.

Two of the three catalytic residues, Tyr22 and Arg17 for *H. pylori* DHQ2, are located in the substrate-covering loop (catalytic loop) that closes the active site after substrate binding (Figure 1 A). It has been shown that the arrangement of the

[a] Dr. A. Peón, A. Robles, Dr. B. Blanco, Prof. C. González-Bello
     Centro Singular de Investigación en Química Biolóxica e Materiais Molecu-
     lares, CIQUS, and Departamento de Química Orgánica, Universidade de
     Santiago de Compostela, calle Jenaro de la Fuente s/n, 15782 Santiago de
     Compostela (Spain)
     E-mail: concepcion.gonzalez.bello@usc.es

[b] Dr. M. Convertino, Prof. A. Caflisch
     Department of Biochemistry, University of Zurich, 8057 Zurich (Switzerland)
     E-mail: caflisch@bioc.uzh.ch

[c] P. Thompson, Prof. A. R. Hawkins
     Institute of Cell and Molecular Biosciences, Medical School, University of
     Newcastle upon Tyne, Catherine Cookson Building, Framlington Place, New-
     castle upon Tyne NE2 4HH (UK)

[d] Dr. M. Convertino
     Current address: Department of Biochemistry and Biophysics, University of
     North Carolina, School of Medicine, Chapel Hill, NC 27599 (USA)

     Supporting information and the ORCID identification number(s) for the
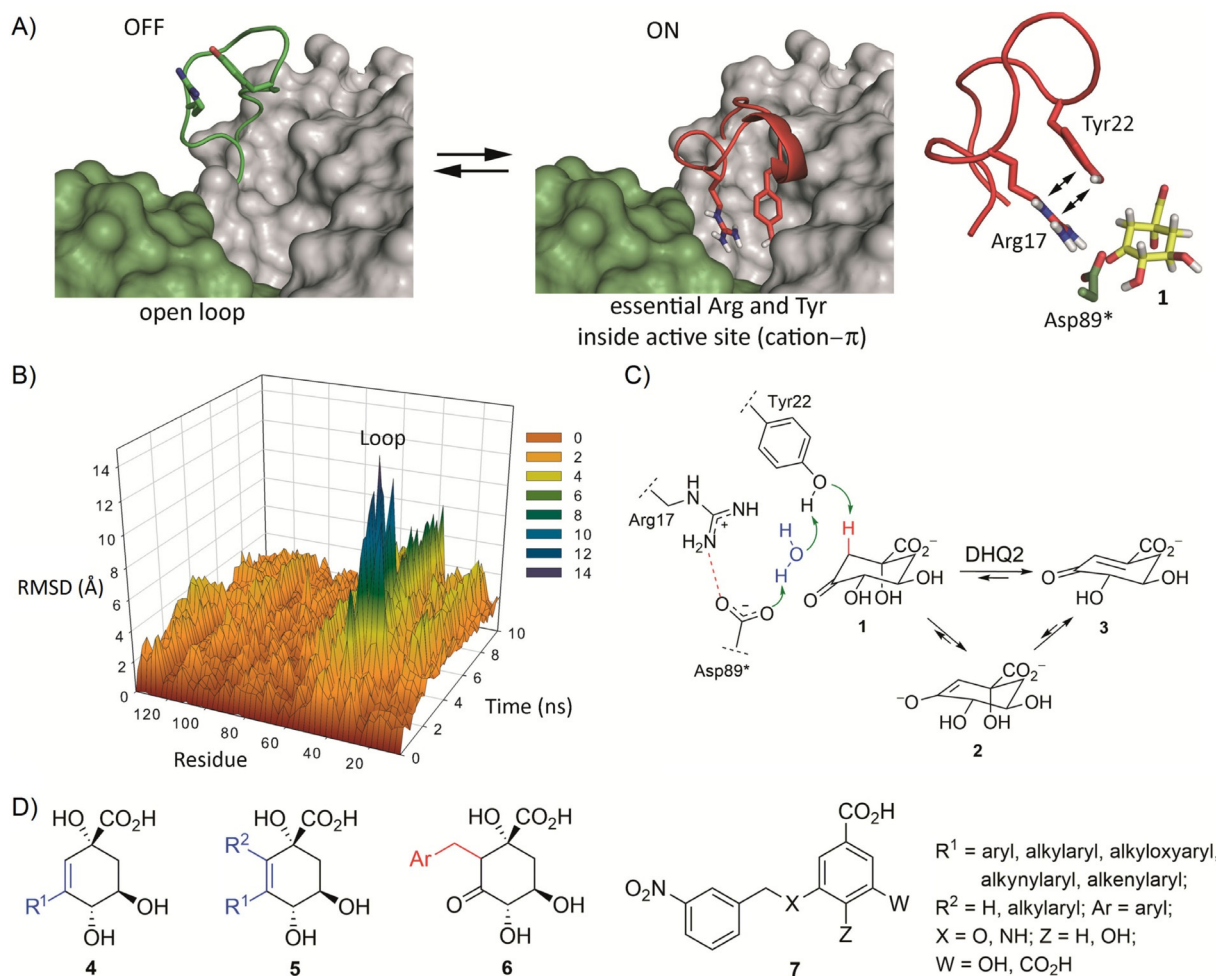   author(s) of this article can be found under:
     https://doi.org/10.1002/cmdc.201700396.

Figure 1. A) Schematic representation of the DHQ2 enzyme motion required for catalysis. Note the cation–π interaction between the essential tyrosine and arginine side chains that are required for catalysis. Both residues must be also pointing toward the active site. Only two chains of the catalytic trimer are shown for clarity. B) RMSD plot for the protein backbone (Cα, C, N, and O atoms) calculated per residue in the DHQ2–**3** complex obtained from MD simulations studies of the product release (DHQ2–**3** enzyme complex).[5] Note how the loop undergoes a large conformational change during product release whereas no significant changes are observed in the rest of the protein. C) Enzymatic conversion of 3-dehydroquinic acid (**1**) into 3-dehydroshikimic acid (**3**) catalyzed by DHQ2; the reaction proceeds via enol intermediate **2**. D) Selected examples of DHQ2 inhibitors.[9–11]

catalytic loop required for catalysis has: 1) the side chains of the tyrosine and arginine residues pointing toward the active site, and 2) a cation–π interaction between the catalytic residues.[5] We believe that targeting the loop plasticity is a good strategy for inhibitor design, because the motion of this loop is an essential process for the DHQ2 catalytic cycle.[5,8] We therefore became interested in designing ligands that are able to alter the flexibility of the loop by compounds structurally different from previously reported compounds, which are mainly based on the mechanism of action.[7] These reported inhibitors are either mimics of the enol intermediate **2**, compounds **4**–**5**,[9] or substrate analogues, compounds **6**[10] (Figure 1D). More recently, several 3-nitrobenzylgallate-based analogues **7** have been described, which incorporate relevant aromatic moieties previously identified by structural and biological studies.[11] Remarkably, in the crystal structure of DHQ2 in complex with the most potent inhibitors is observed that the aromatic moiety present in their structure block the entrance of the essential arginine side chain into the active site and

cause an important change in the appropriate arrangement and flexibility of the substrate-covering loop.[12] These aromatic moieties are located in the interface pocket, which separates two neighbor subunits of the enzyme and is located at the entrance of the active site. DHQ2 is a dodecamer formed from a tetramer of trimers, a trimer being the minimum catalytic unit of the enzyme.[13] QSAR studies also revealed that this pocket is key for the efficacy and specificity of inhibitors.[14,15]

In particular, we aimed for ligands that would either stabilize the closed form avoiding the entrance of the substrate or the open conformation providing a widely exposed active site. For our goal, we took into account: 1) our previous studies on the motion of the catalytic loop during product release pinpointed by molecular dynamics (MD) simulation studies of the product enzyme complex (Figure 1B),[5] 2) the loop conformational changes observed in the crystal structures of DHQ2 from *M. tuberculosis* (*Mt*-DHQ2) and *H. pylori* (*Hp*-DHQ2) in complex with some of the most potent reported inhibitors,[6] and 3) the well-

established advantages of the fragment-based approaches, as discussed below.[16–25]

We aim to identify inhibitors containing drug-like entities that might facilitate the entrance into the bacterium cell in which the aromatic fragments would be located in the interface pocket to block the active site entrance. For this purpose, fragment-based screening is nowadays a wide accepted technique to identify relatively simple hit-compounds that possess a high binding affinity per heavy atom, and thus are ideal compounds for optimization into clinical candidates with good drug-like properties.[16–25] This technique has emerged as an important alternative to high-throughput screening,[24,25] because it has the advantage that incorporates the structural information[26] of the target to preselect the molecules that are most likely to show binding and inhibitory activity. The available experimental knowledge of known inhibitors is incorporated by using pharmacophore constraints to preselect compounds for docking and therefore decreasing computation times. Computer-aided fragment-based approaches are being increasingly proven as a successful means of generating novel hits for drug discovery programs.[27] In this context, the Anchor-based Library Tailoring screening Approach (ALTA), which was developed in 2008 by Caflisch et al.,[28] has proven to be very efficient for the discovery of novel inhibitors of a variety of targets. For instance, it has been successfully applied to the discovery of inhibitors of tyrosine kinase erythropoietin producing human hepatocellular carcinoma receptor B4,[28,29] of the West Nile virus NS3 protease,[30] cathepsin B,[31] the human cyclin-dependent kinase 2[32] and several human bromodomains.[33] The essential element of the ALTA method is the use of optimally docked small fragments to select from a large library of compounds only those that have one (or more) of the top-ranking fragments.

Herein we present the computer-aided fragment-based identification of reversible competitive inhibitors of a recognized target for antibiotic drug discovery, *Hp*-DHQ2. The synthesis of the identified potential compounds and their inhibitory activity are also provided. Moreover, chemical modifications on the most active compound obtained in this study were also explored for further optimization. We provide evidence based on MD simulation studies that our inhibitors decrease the plasticity of the catalytic loop by blocking key residues for the catalysis.

Results and Discussion

Fragment-based identification of ligands

The subset "clean-leads" of the ZINC database[34] with about 1.5 million compounds was chosen for this study. The computer-aided fragment-based approach used, ALTA, involves four consecutive steps (Figure 2): 1) automatic decomposition of each molecule of the chemical library into fragments using the program DAIM (Decomposition And Identification of Molecules),[35] 2) fragment docking using SEED (Solvation Energy for Exhaustive Docking) for selection and ranking of the fragments,[36] 3) substructure search of the ALTA-selected frag-
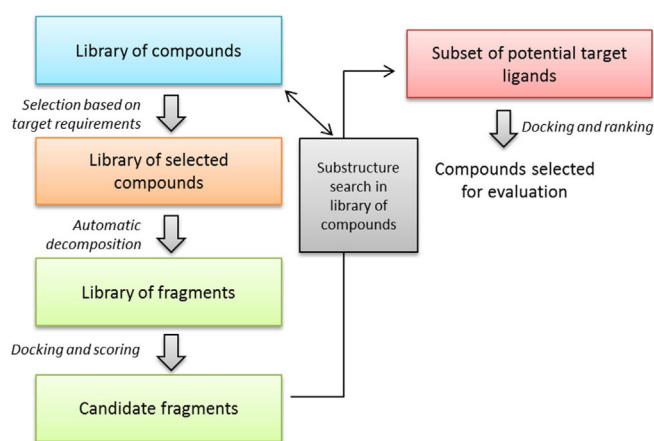

Figure 2. Graphical representation of the ALTA procedure workflow.

ments into the chemical library for initial selection of potential ligands, and 4) flexible docking of each selected compound using the best poses of its fragments as anchors for final compound selection and ranking. This is carried out using FFLD[37] (Fast Flexible Ligand Docking) and CHARMM[38] for the energy minimization of the resulting enzyme–ligand complex. Evaluation of the binding free energy of multiple poses of each compound makes use of the LIECE (Linear Interaction Energy with Continuum Electrostatics) method.[39]

To discard at an early stage fragments that are unlikely to bind, several pharmacophores constraints were used. In particular, considering that the active site of DHQ2 has several residues capable of recognizing bidentate groups such as carboxylates or sulfonamides, a filtering step discarded all compounds devoid of these functional groups. It was also considered that compounds should have a maximum of 10 rotatable bonds, between 2 and 6 acceptor groups, ≤ 3 donor groups, and a total number of hydrogen-bond acceptors and donors of ≤ 10. As a consequence, the chemical library was decreased to 239 779 compounds, from which DAIM extracted 61 549 candidate fragments.

Docking was carried out using the previously reported enzyme structure of *Hp*-DHQ2 in complex with (1*R*,4*S*,5*R*)-1,4,5-trihydroxy-3-[(5-methyl-1-benzothiophen-2-yl)methoxy]cyclohex-2-ene-1-carboxylic acid (**4a**, [1]R = (5-methyl-1-benzothiophen-2-yl)methoxy), PDB ID: 2WKS).[9m] This crystal structure was chosen because it has an inappropriate conformation of the substrate-covering loop for catalysis. Thus, the aromatic moiety in **4a** expels the side chain of the essential Arg17 out of the active site and, under this arrangement the enzyme is efficiently inhibited. After fragment docking, the library of fragments was reduced to 10 712 candidate fragments. Using all these fragments as queries a subset of 30 309 compounds from the initial library was generated. After flexible docking of each molecule of the library using the best poses of its fragments as anchors, the best 50 top-ranking compounds were selected (Table S1). The first two compounds and seven of the remaining ones, which were selected based on structural considerations of the key interactions with the enzyme, were chosen for biological evaluation (Figure 3). Compounds **8** and
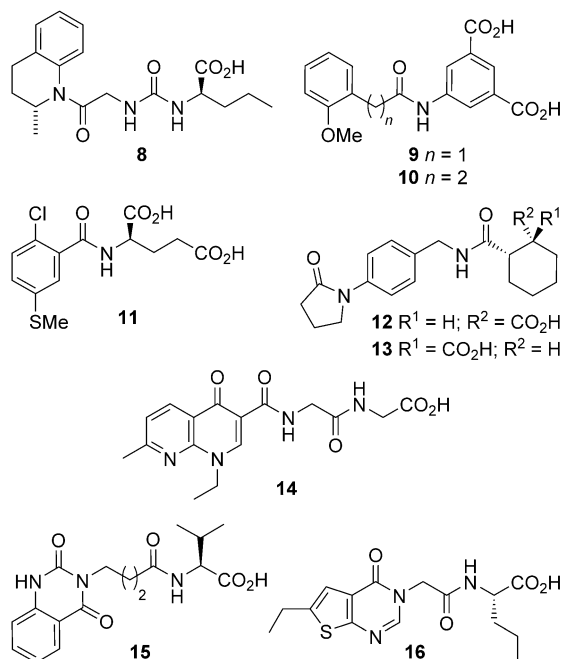
Figure 3. Selected potential inhibitors of the *Hp*-DHQ2 enzyme obtained by the fragment-based approach.

15–**16** were obtained from commercial sources and compounds **9**–**14** were synthesized using standard procedures (see a detailed description in the Supporting Information).

Inhibitory activity of compounds 8–16

The potential DHQ2 ligands identified by ALTA-approach, compounds **8**–**16**, were assayed in the presence of 3-dehydroquinic acid (**1**) for their inhibitory properties against *Hp*-DHQ2. The inhibition data are summarized in Table 1. In general, these compounds were found to be reversible competitive inhibitors of the enzyme with K_i values in the micromolar range, below the K_M of the enzyme. The most potent inhibitor proved to be the quinazolinedione **15** with a K_i of 19 μM. This compound clearly stands out from the series, as the next, specifically compounds **9**, **14**, and **16**, showed K_i values between 77 and 91 μM.

Table 1. K_i values for compounds **8**–**16** against *Hp*-DHQ2.[a]

Compound	K_i [μM][b]
8	141 ± 19
9	77 ± 5
10	139 ± 12
11	103 ± 13
12	159 ± 15
13	> 300
14	85 ± 5
15	19 ± 2
16	91 ± 12

[a] Assay conditions: Tris·HCl (50 mM), pH 7.0, 25 °C; K_M (**1**) = 444 μM. [b] Values are the mean ± SEM of $n = 3$ determinations.

Binding mode of compounds 8–16

The binding modes of the most potent identified inhibitors, compounds **9** and **14**–**16**, revealed that the aromatic ring of the ligands **9** and **14**–**16** would be located in the interface pocket (Figure 4). The aromatic moiety of compounds **9** and **14**–**16** should have apolar interactions with the side chain of Leu93*, Met92* and the carbon side chain of Asp89* (residues from this subunit are marked with an asterisk). The essential Asp89* proved to be responsible for the deprotonation of the essential Tyr22 to afford the catalytic tyrosinate, which in turn triggers the enzymatic process.[5] Moreover, several lipophilic interactions with the side chain of Leu11 and Leu14 were also recognized.

The carboxylate group of the inhibitors would be located in the C1 binding pocket by forming hydrogen-bonding interactions with the side chain of Asn76, the main amide chain of Leu103 and Thr104. This pocket has been proven to be crucial for substrate recognition and enzyme catalysis.[40] Thus, the carboxylate group of the natural substrate interacts with the active site through four strong hydrogen bonds involving the main chain NH amide group of Leu103 and Thr104, the OH group of the side chain of Thr104 side chain and the amide side chain of Asn76 (Figure S1). Moreover, two hydrogen bonds with the conserved Asn76 and His102 is the way in which the enzyme controls the correctly positioning of the C1 hydroxy group for the final elimination step.

Remarkably, in addition to the above mentioned interactions, the binding modes of the most active inhibitors appear to have in common π–π stacking and hydrogen-bonding interactions with Tyr22. Specifically, a hydrogen bond between the phenol group of Tyr22 and the amide carbonyl group of ligand **9** or the carbonyl group of the aromatic ring of ligands **14**–**16** would take place. Tyr22 is the essential residue that removes the pro-*R* hydrogen of C2 in **1** and which appropriate orientation for catalysis is controlled by the essential Arg17. This hydrogen-bonding interaction with Tyr22 is absent in the weakest inhibitors of the series, ligands **8** and **10**–**12**, (Figure S2). In addition, the predicted binding of ligands **8** and **12** would be very different from the rest of the tested ligands in this study, which might explain its lower potency. However, in both cases, the aromatic ring of the ligands would be located in the interface pocket. Once the aromatic ring is fixed in this region, the rest of the molecule seems to be located in the space available of the active site by establishing hydrogen-bonding interactions with polar residues of the active site. These results revealed that a large number of the aromatic moieties included in the reported ligands are well located in the interface pocket and might therefore be good hit fragments to be considered in future designs.

In general: 1) ligand **14** would be the only one lacking any interactions with the C6–C5 substrate recognition center of the enzyme involving the conserved residue His82; 2) the interaction of the aromatic moiety with the essential Tyr22 and the interface pocket in **16** seems to be less efficient than for compounds **9** and **14**–**15**; and 3) compound **15** would be the ligand that would best interact with the main pockets of the
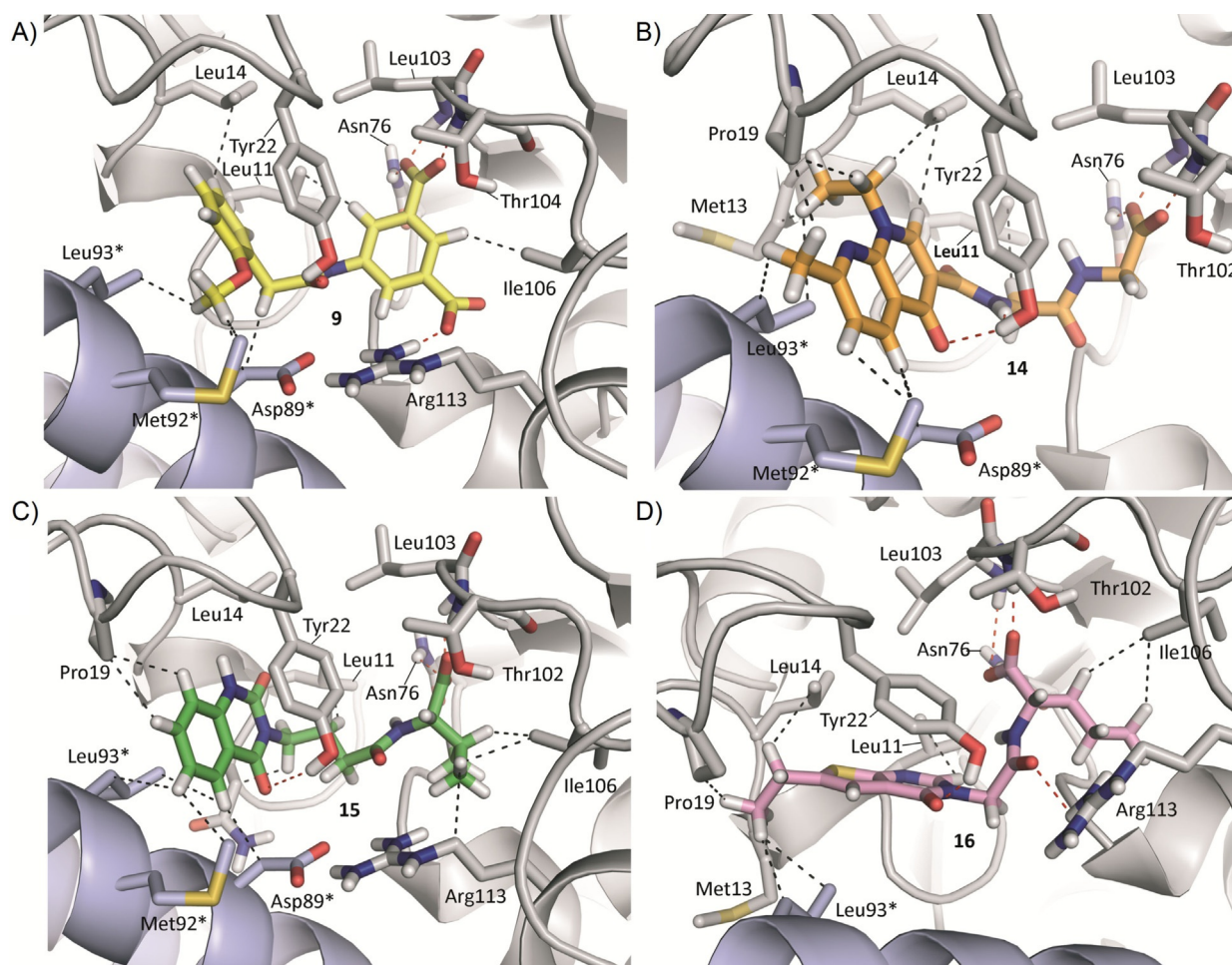
Figure 4. Selected view of the predicted binding mode of ligands: A) **9** (yellow), B) **14** (orange), C) **15** (green), and D) **16** (pink) in the *Hp*-DHQ2 active site. The neighboring chain close to the active site is shown in blue and its relevant side chain residues are indicated with an asterisk. Relevant side chain residues are shown and labeled. Hydrogen-bonding (red) and lipophilic (grey) interactions are indicated as dashed lines.

enzyme, which might explain its higher inhibitory potency. Moreover, considering that ligand **9** is structurally very close to 3-nitrobenzylgallate-based analogues **7**, which were reported by Abell et al.[11] during the realization of the herein presented studies, our subsequent efforts were focused on the optimization of ligand **15**.

Globally, the most potent inhibitor identified in this study, compound **15**, contains two key moieties: 1) the quinazoline-dione ring and 2) the carboxylate group. Among the two, the aromatic ring seems to be particularly well located to reduce the flexibility of the substrate-covering loop by interaction with the essential tyrosine and the interface pocket. Hence, to explore the possible improvement of the inhibitory activity obtained, the modification of the chain containing the carboxylate group in **15** was then studied.

Four new quinazolinedione derivatives—compounds **17S**, **17R**, and **18** and **19**—were designed (Figure 5 A). We took into account the binding mode of citrate in the crystal structure of *Hp*-DHQ2–citrate binary complex (PDB ID: 2C4V, 2.5 Å) reported by Lapthorn et al.[41] This compound proved to be a competitive inhibitor of the enzyme with a K_i value of 2.5 mM. Compounds **17S** and **17R** containing an acetate group instead

of an isopropyl one were designed to improve the interaction with the conserved His82, which is involved in the recognition of the C5 hydroxy group.

In addition, reasoning that in the Michaelis complex the C1 hydroxy group interacts by hydrogen bonding with the conserved Asn76 and His102 to correctly positioning this group in the final elimination step (Figure S1),[5] the incorporation of a tertiary hydroxy group was also explored with compound **18**. Finally, considering that the amide linker does not seem to interact with the enzyme active site residues, the effect of the incorporation of a flexible carbon chain was explored with compound **19**.

Chain optimization: quinazolinedione derivatives 17–19

Synthesis

Compounds **17** and **18** were prepared by amide coupling between the acids **26** and **30** and the amines dimethyl L-aspartate, dimethyl D-aspartate, and **24**, respectively (Figure 5 B). Our initial efforts for the synthesis of the aminoquinazoline-dione **24** involved the nucleophilic substitution of commercial-
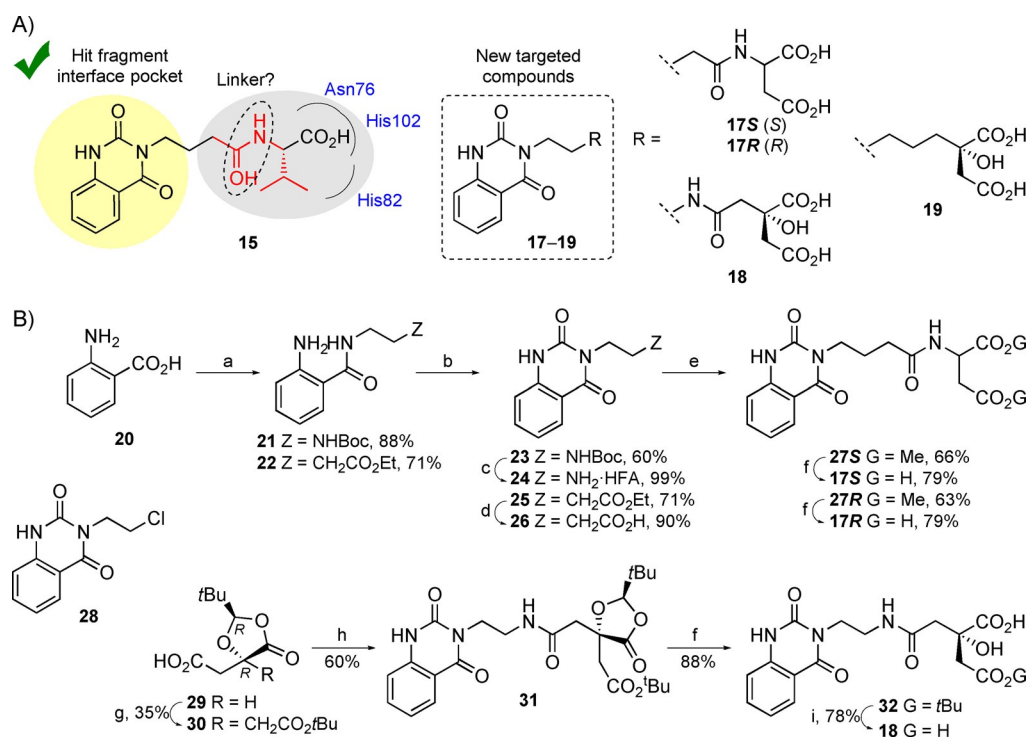
Figure 5. A) Explored chemical modifications of the carboxylate containing chain in **15**, and new targeted quinazolinedione derivatives **17–19**. B) Synthesis of compounds **17S**, **17R** and **18**. *Reagents and conditions*: a) N-Boc-ethylenediamine (for **21**) or ethyl 4-aminobutaroate (for **22**), EDC, DMAP, DMF, RT; b) triphosgene, DIPEA, CH_2Cl_2, RT; c) TFA, CH_2Cl_2, 0 °C; d) 1. LiOH, THF, RT, 2. HCl (10%); e) 1. $SOCl_2$, 60 °C, 2. dimethyl L-aspartate (for **27S**) or dimethyl D-aspartate (for **27R**), Et_3N, CH_2Cl_2, RT; f) 1. LiOH, 2. Amberlite IR-120 (H$^+$); g) 1. LHMDS, THF, −78 °C, 2. $BrCH_2CO_2tBu$, −23 °C; h) **24**, HATU, DIPEA, DMF, RT; i) HCl (4.5 M), RT.

ly available chloride **28** with lithium amide, sodium azide or benzylamine, various solvents (DMF, MeCN, Toluene), bases (K_2CO_3, DIPEA) and reaction temperatures (50–100 °C). However, all the attempts afforded mainly starting material or an intramolecular cyclization reaction of **28**. The synthesis of the amino **24** was finally achieved in three steps from anthranilic acid (**20**) by first incorporation of the required chain followed by quinazolinedione ring formation. Thus, EDC condensation with commercially available N-Boc-ethylenediamine followed by intramolecular condensation of the resulting amide **21** with triphosgene and subsequent removal of the Boc protecting group in **23** with TFA yielded the required amine **24** as trifluoroacetic acid salt. Following a similar strategy, the quinazolinedione **26** was prepared from ethyl 4-aminobutaroate and anthranilic acid (**20**).

On the other hand, the required acid **30** for the preparation of **18** was synthesized following Seebach's[42] self-reproduction of chirality synthetic principle. Thus, alkylation with *tert*-butyl bromoacetate of the carbanion resulting of the treatment with lithium hexamethylsilazide of previously reported dioxolanone acid **29**[43] afforded the desired compound **30**. Next, amide coupling between the acids **26** and **30** and the amines dimethyl L-aspartate, dimethyl D-aspartate and **24**, respectively, using HATU as coupling agent and in the presence of diisopropylethylamine gave the amides **27S**, **27R** and **31**, respectively. Finally, deprotection of latter compounds yielded the required amides **17S**, **17R** and **18**, respectively.

The synthesis of compound **19**, in which the quinazolinedione and the carboxylic acid moieties are linked through a sa-

turated carbon chain, proved to be more challenging. An olefin cross-metathesis (OCM) approach involving the construction of the C4–C5 carbon bond was designed (Scheme 1A). This disconnection was chosen because it would allow the use of the allyl derivative **34**,[43] which is readily prepared by alkylation with allyl bromide of the dioxolanone acid derived from L-malic acid, compound **35**. Initial alkylation attempts revealed that the use of less reactive electrophiles such as long chain alkyl bromides provide quite low yields of the required products.

All the attempts of OCM between the allyl derivatives **33** and **34** revealed to be unsatisfactory due to the poor selectivity toward the required heterodimer product. Homodimerization of **34** was the main reaction product whereas compound **33** showed to have very low reactivity. Fortunately, the selectivity toward the heterodimer product was achieved following the general guidelines reported by Grubbs et al.[44] consisting in the use of two olefins of remarkably different reactivity (Scheme 1B). Thus, the OCM between 4-bromobutene (type I olefin) and compound **34** (type II olefin) catalyzed by second generation of Grubbs–Hoyveda catalysts gave the cross *trans*-olefin **36** in 71% yield.

Having incorporated the carbon long chain, the following steps were focused in the construction of the quinazolinedione ring. First, the bromide **36** was converted into the required amine by nucleophilic substitution with sodium azide and subsequent Staudinger reduction of the resulting azide **37**. The EDC-coupling of the terminal amine with anthranilic acid (**20**) in the presence of 4-N,N-dimethylpyridine gave the amide **38**.
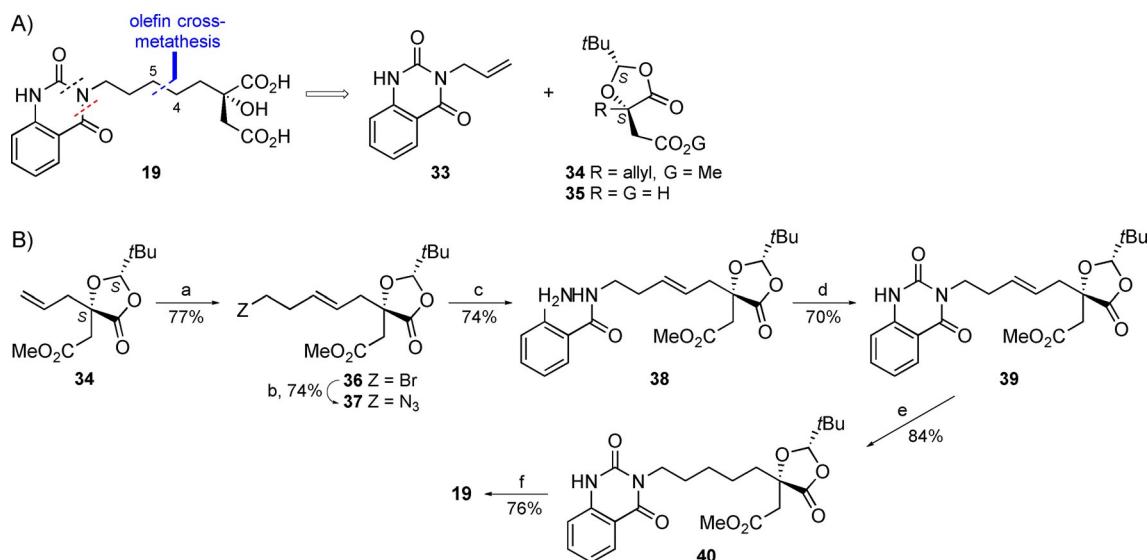
Scheme 1. A) Explored olefin cross-metathesis strategy for the synthesis of **19**. B) Synthesis of compound **19**. *Reagents and conditions*: a) 4-bromobutene, Grubbs–Hoveyda 2nd-generation catalyst, PhMe, 90 °C; b) NaN₃, DMF, 90 °C; c) 1. Ph₃P, THF, H₂O, Δ, 2. 20, EDC, DMAP, RT; d) triphosgene, Et₃N, CH₂Cl₂, RT; e) H₂, Pd/C (10 %), EtOH, RT; f) 1. LiOH, 2. Amberlite IR-120 (H⁺).

It is important to highlight that the presence of a *trans* double bond in the carbon chain is key for the successful synthesis of the aromatic ring. Thus, the conformational restriction induced by this olefin avoids the intramolecular nucleophilic attack by the resulting amine to the methyl ester. Finally, the intramolecular condensation of **38** with triphosgene gave the quinazolinedione **39** that was transformed into the desired compound **19** by catalytic hydrogenation of the double bond and subsequent hydrolysis of the resulting saturated compound **40**.

Inhibitory activity of compounds 17–19 and 32

The results of inhibition activity of compounds **17–19** and **32** against *Hp*-DHQ2 revealed that decreasing the conformational restriction in the carbon bearing the carboxylic group, which is involved in the recognition in the C1 pocket, enhances the inhibitory potency (Table 2). The most favorable effect was achieved with compound **19** ($K_i = 6.3$ μM) having a flexible carbon chain. In addition, it seems that the increased flexibility also favors extra interactions of the incorporated tertiary hydroxy and acetate groups with residues Asn76, Leu103, His102 and His82, as designed. In fact, no significant effects were observed

when the latter groups were introduced in the ligand having an amide linker, compound **18**. To corroborate this hypothesis, to assess the reliability of the proposed complexes, and to determine the conformational changes caused in the substrate-covering loop of *Hp*-DHQ2 after compound **19** binding, MD simulations studies were conducted with the highest score solutions obtained by docking for ligands **18** and **19**.

MD simulations

The binding modes of ligands **18** and **19** were first generated by the program GOLD[45] version 5.2 using the same enzyme structure as for the fragment docking, i.e., PDB ID: 2WKS.[9m] The highest score solution for the two *Hp*-DHQ2–**18** and *Hp*-DHQ2–**19** binary complexes were subjected to 100 ns of MD simulations at a temperature of 300 K (Figure 6). These studies were carried out considering a dual protonation of His102 based on mechanistic reasons and the three possible protonation states of His82, that is, dual (δ and ε) and single (δ or ε). The best results were obtained with a dual protonation of His82 because in doing so the carboxylate group is well stabilized nearby. Other protonation states provided significant motion on the His82 side chain. In addition, similar results were obtained from MD simulation studies on the *Hp*-DHQ2–citrate binary complex (PDB ID: 2C4V). These results explain why in the latter structure the electronegative O4 atom of one of the carboxylate group in citrate is located at 2.5 Å of the also electronegative Nε1 atom of His82 residue.

The results clearly show that the flexible carbon chain in **19**: 1) causes a more pronounced decrease in the flexibility of the catalytic loop than in **18** and 2) enhances the strength of the hydrogen bonding interactions involving residues Asn76, His102, Leu103 and His82. These effects are easily visualized by analyzing the variation of the distance between the atoms involved in these hydrogen bonds during the 100 ns of simula-
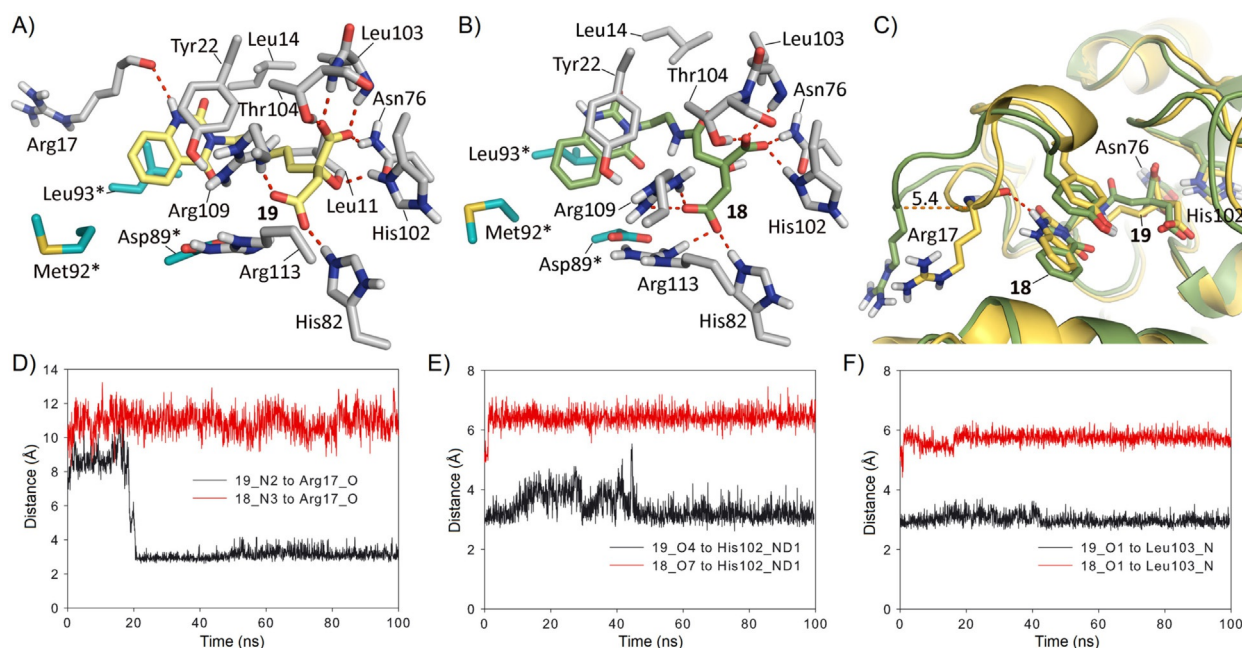
Table 2. K_i values for compounds 17–19 and 32 against *Hp*-DHQ2.[a]	
Compound	K_i [μM][b]
15	19 ± 2
17S	111 ± 3
17R	52 ± 5
18	18 ± 2
19	6.3 ± 0.2
32	166 ± 15
[a] Assay conditions: Tris·HCl (50 mM), pH 7.0, 25 °C; K_M (**1**) = 444 μM. [b] Values are the mean ± SEM of $n = 3$ determinations.	

Figure 6. Detailed view of the predicted binding of ligands **19** (A, yellow) and **18** (B, green) in the active site of *Hp*-DHQ2 obtained by MD simulation studies. Both poses showed correspond to snapshots after 60 ns of MD simulation. Hydrogen-bonding interactions between ligand and several residues of the active site are shown as red dashes. C) Comparison of the binding mode of ligands **19** and **18** in the active site of *Hp*-DHQ2. D)–F) Variation of the relative distance between resides Arg117 (O atom, D), His102 (Nδ1 atom, E), and Leu103 (N atom, F) and NH group of the aromatic moiety (N2 and N3 atoms), the medium chain carboxylate (O4, O7 and O1 atoms) in **19** and **18**, respectively, during the whole simulation. Note how ligand **19** has stronger hydrogen bonding interactions with the latter residues than ligand **18** and provides a closer and more organized conformation of the substrate-covering loop. Side chain residues from the neighbor chain are shown in cyan and labeled with an asterisk.

tion (Figures 6 E,F and S3). Thus, for ligand **19**, the loop folds on top of the ligand so that after 20 ns of simulation a stable hydrogen bond between the NH group of the aromatic moiety and the backbone carbonyl of Arg17 (in the catalytic loop) is formed with an average distance of 3.1 Å (distances are measured between heavy atoms; Figures 6 C,D). In fact, our MD studies revealed that in the presence of **19** the loop is clearly more ordered (Figure 6 C). After the folding, the complex is very stable as no significant changes were observed for the remaining simulation (Figure S4 A). This phenomenon was not observed for ligand **18**, showing an average distance of 10.9 Å. The *Hp*-DHQ2–**18** complex remained unchanged during the whole simulation (Figure S4 B).

Moreover, the hydrogen bonds between the hydroxy and carboxylate groups in **19** with the NH groups of His102, Asn76 and Leu103 have an average distance of 3.4 Å and 3.0 Å, respectively. For **18**, they are 6.4 Å and 5.7 Å, respectively. Therefore, the incorporation of the flexible chain in **19** seems to enhance the binding of the carboxylate group of the inhibitor in the C1 recognition center. The strength of hydrogen bonds involving residue His82 are quite similar (Figure S3). For both ligands, the terminal carboxylate group would interact by favorable electrostatic interactions with the conserved residues Arg109, Arg113 and His82.

Conclusions

A multidisciplinary approach has been used here to search for ligands able to disable the enzyme flexibility that is an essential process for catalysis. This has been applied to the inhibition of a recognized target for antibiotic discovery, the type II dehydroquinase from *Helicobacter pylori* (*Hp*-DHQ2), which is essential enzyme in this pathogenic bacterium. A computer-aided fragment-based approach, ALTA, was first used to identify the aromatic fragment able to block the active site entrance by binding to the interface pocket that separates two neighbor enzyme subunits. The identified quinazolinedione **15** proved to be a reversible competitive of the *Hp*-DHQ2 with a K_i of 19 μм, below the K_M of the enzyme (444 μм). Subsequent chemical modification of the non-aromatic moiety in **15** through an olefin cross-metathesis and Seebach's self-reproduction of chirality synthetic principle allowed the development of a quinazolinedione derivative containing a flexible malate moiety, compound **19**, that seems to efficiently disables the enzyme motion. The latter ligand proved to be more potent with a K_i of 6.3 μм. The results from our MD simulation studies revealed that favoring the geometric perfection in anchoring the ligand at the center C1 recognition center, the motion of the loop would be frozen by the aromatic fragment and consequently the effective inhibition of the enzyme is achieved. This would be accomplished by π–π stacking interaction between the fragment and the catalytic tyrosine and by hydrogen bonding with the main amide group of the essential arginine. In doing so, the position of both residues would be well fixed in an inappropriate arrangement for catalysis. We also believe that some of the fragments identified in this work might be also useful hit fragments for future designs if the interaction with the C1 carboxylate pocket is improved.

Experimental Section

Experimental details regarding the synthesis of compounds **9**–**14** are provided in the Supporting Information.

2-Amino-N-[2-(N-Boc)aminoethyl]benzamide (21): An stirred solution of anthranilic acid (**20**) (100 mg, 0.73 mmol) and N-Boc-ethylenediamine (0.17 mL, 1.09 mmol) in dry DMF (3.6 mL), under argon and at room temperature, was treated with EDC (168 mg, 0.87 mmol) and N,N-dimethylpyridine (4.4 mg, 0.04 mmol). The resulting mixture was stirred at room temperature for 12 h. The reaction mixture was diluted with ethyl acetate and water. The organic layer was separated and the aqueous phase was extracted with ethyl acetate (×2). The combined organic layers were dried (anh. Na_2SO_4), filtered and concentrated under reduced pressure. The residue obtained was purified by flash chromatography, eluting with (60:40) ethyl acetate/hexane, to give the amide **21** (179 mg, 88%) as a white solid; mp: 163–164 °C; ^{1}H NMR (300 MHz, CDCl$_3$): $\delta = 7.37$ (d, $J = 7.8$ Hz, 1H, ArH), 7.22–7.14 (m, 1H, ArH), 6.98 (br s, 1H, NH), 6.63 (m, 2H, 2×ArH), 5.54 (br s, 2H, 2×NH), 5.04 (br s, 1H, NH), 3.56–3.43 (m, 2H, CH$_2$), 3.37 (m, 2H, CH$_2$) and 1.42 ppm (s, 9H, C(CH$_3$)$_3$); ^{13}C NMR (75 MHz, CDCl$_3$): $\delta = 170.0$ (C), 157.4 (C), 148.9 (C), 132.4 (CH), 127.6 (CH), 117.4 (CH), 116.7 (CH), 115.7 (C), 80.0 (C(CH$_3$)$_3$), 41.5 (CH$_2$), 40.2 (CH$_2$) and 28.5 ppm (C(CH$_3$)$_3$); IR (ATR): $\tilde{v} = 3445$ (NH), 3349 (NH), 1674 (CO) and 1620 cm^{-1} (CO); MS (ESI) m/z: 302 [M+Na]$^+$; HRMS calcd for C$_{14}$H$_{21}$N$_3$O$_3$Na [M+Na]$^+$: 302.1475, found: 302.1483.

Ethyl 4-(2-aminobenzamido)butanoate (22): A solution of ethyl 4-aminobutaroate (1 g, 5.96 mmol) and dry triethylamine (0.9 mL, 5.96 mmol) in dry dichloromethane (52 mL) and under inert atmosphere was treated at room temperature with EDC (1.26 g, 6.56 mmol) and anthranilic acid (**20**) (2.3 g, 11.92 mmol) in three portions during 1.5 h. The reaction mixture was washed with aqueous sodium bicarbonate. The organic phase was separated and the aqueous layer was extracted with dichloromethane (×2). The combined organic extracts were dried (anh. Na_2SO_4), filtered and concentrated under reduced pressure. The residue obtained was purified by flash chromatography, eluting with (95:5) dichloromethane/ethyl acetate, to give the amide **22** (782 mg, 71%) as an orange oil. ^{1}H NMR (250 MHz, CDCl$_3$): $\delta = 7.24$ (dd, $J = 7.8$ and 1.5 Hz, 1H, ArH), 7.06 (td, $J = 1.5$ and 7.0 Hz, 1H, ArH), 6.73 (br s, 1H, NH), 6.55 (dd, $J = 8.1$ and 1.1 Hz, 1H, ArH), 6.49 (td, $J = 1.5$ and 8.0 Hz, 1H, ArH), 5.22 (br s, 2H, NH$_2$), 4.00 (q, $J = 7.1$ Hz, 2H, OCH$_2$), 3.30 (q, $J = 6.5$ Hz, 2H, NCH$_2$), 2.28 (t, $J = 7.1$ Hz, 2H, COCH$_2$), 1.79 (quint, $J = 7.0$ Hz, 2H, NCH$_2$CH$_2$) and 1.13 ppm (t, $J = 7.1$ Hz, 3H, CH$_3$); ^{13}C NMR (63 MHz, CDCl$_3$): $\delta = 173.5$ (C), 169.4 (C), 148.5 (C), 131.9 (CH), 127.2 (CH), 117.0 (CH), 116.3 (CH), 115.9 (C), 60.4 (OCH$_2$), 39.0 (NCH$_2$), 31.7 (CH$_2$), 24.4 (CH$_2$) and 14.0 ppm (CH$_3$); IR (ATR): $\tilde{v} = 3192$ (NH), 1719 (CO) and 1625 cm^{-1} (CO); MS (ESI) m/z: 251 [M+H]$^+$; HRMS calcd for C$_{13}$H$_{19}$N$_2$O$_3$ [M+H]$^+$: 251.1390, found: 251.1385.

3-[2-(N-Boc)aminoethyl]quinazoline-2,4(1H,3H)-dione (23): A suspension of amide **21** (89 mg, 0.32 mmol) and triphosgene (47 mg, 0.16 mmol) in dry dichloromethane (1.6 mL), under argon and at room temperature, was treated with DIPEA (0.1 mL, 0.64 mmol) and the resultant solution was stirred for 1 h. The reaction mixture was diluted with dichloromethane and saturated aqueous solution of NaHCO$_3$. The aqueous layer was separated and the organic phase was washed with water. The organic extract was dried (anh. Na_2SO_4), filtered and concentrated under reduced pressure. The residue obtained was purified by flash chromatography, eluting with (75:25) ethyl acetate/hexane, to give the quinazolinedione **23** (58 mg, 60%) as a white solid; mp: 204–205 °C; ^{1}H NMR (300 MHz, [D$_6$]DMSO): $\delta = 11.35$ (br s, 1H, NH), 7.92 (dd, $J = 7.9$ and 1.1 Hz, 1H, ArH), 7.65–7.60 (m, 1H, ArH), 7.20–7.14 (m, 2H, 2×ArH), 6.82 (t, $J = 5.8$ Hz, 1H, NH), 3.97 (t, $J = 5.8$ Hz, 2H, CH$_2$), 3.19 (t, $J = 5.8$ Hz, 2H, CH$_2$) and 1.28 ppm (s, 9H, C(CH$_3$)$_3$); ^{13}C NMR (63 MHz, [D$_6$]DMSO): $\delta = 162.2$ (C), 155.8 (C), 150.4 (C), 139.6 (C), 134.8 (CH), 127.4 (CH), 122.3 (CH), 115.0 (CH), 114.0 (C), 77.5 (C(CH$_3$)$_3$), 40.2 (CH$_2$), 37.7 (CH$_2$) and 28.2 ppm (C(CH$_3$)$_3$); IR (ATR): $\tilde{v} = 3372$ (NH), 1703 (CO), 1671 (CO) and 1648 cm^{-1} (CO); MS (ESI) m/z: 328 [M+Na]$^+$; HRMS calcd for C$_{15}$H$_{19}$N$_3$O$_4$Na [M+Na]$^+$: 328.1268, found: 328.1262.

3-(2-Aminoethyl)quinazoline-2,4(1H,3H)-dione trifluoroacetic acid salt (24): A suspension of protected amine **23** (50 mg, 0.16 mmol) in dichloromethane (1.3 mL) at 0 °C was treated with TFA (1.3 mL) and the resultant solution was stirred for 3 h. The reaction mixture was diluted with dichloromethane and water. The organic phase was separated and the aqueous phase was washed with dichloromethane. The aqueous extract was lyophilized to give the amine trifluoroacetic acid salt **24** (50 mg, 99%) as a white solid; mp: 253–255 °C; ^{1}H NMR (300 MHz, CD$_3$OD): $\delta = 8.03$ (dd, $J = 7.9$ and 1.0 Hz, 1H, ArH), 7.67–7.62 (m, 1H, ArH), 7.20–7.25 (m, 1H, ArH), 7.17 (d, $J = 8.2$ Hz, 1H, ArH), 4.32 (t, $J = 5.5$ Hz, 2H, CH$_2$) and 3.26 ppm (t, $J = 5.5$ Hz, 2H, CH$_2$); ^{13}C NMR (63 MHz, CD$_3$OD): $\delta = 165.3$ (C), 153.1 (C), 141.4 (C), 137.0 (CH), 129.3 (CH), 124.6 (CH), 116.7 (CH), 115.9 (C), 40.4 (CH$_2$) and 39.9 ppm (CH$_2$); IR (film): $\tilde{v} = 3014$ (NH), 1720 (CO), 1687 (CO) and 1654 cm^{-1} (CO); MS (ESI) m/z: 204 [M−H]$^-$; HRMS calcd for C$_{10}$H$_{10}$N$_3$O$_2$ [M−H]$^-$: 204.0779, found: 204.0782.

Ethyl 3-(2,4-dioxo-1,4-dihydroquinazolin-3(2H)-yl)propanoate (25): A solution of the amine **22** (50 mg, 0.26 mmol) and triethylamine (72 μL, 0.52 mmol) in dry dichloromethane (1.3 mL), under inert atmosphere and at room temperature, was treated with a solution of triphosgene in dry dichloromethane (0.3 mL, 0.16 mmol, 0.2 M). The resulting solution was stirred for 2 h and then washed with HCl (10%, ×3). The aqueous phase was extracted with dichloromethane (×3). The combined organic extracts were dried (anh. Na$_2$SO$_4$), filtered and concentrated under reduced pressure. The residue obtained was purified by flash chromatography, eluting with (40:10) diethyl ether/hexane, to give the quinazolinedione **25** (51 mg, 71%) as a yellow solid; mp: 270–271 °C; ^{1}H NMR (250 MHz, CDCl$_3$): $\delta = 10.85$ (br s, 1H, NH), 8.07 (d, $J = 7.8$ Hz, 1H, ArH), 7.61 (td, $J = 1.3$ and 8.2 Hz, 1H, ArH), 7.20 (m, 2H, 2×ArH), 4.12 (t, $J = 6.8$ Hz, 2H, NCH$_2$), 4.05 (q, $J = 7.1$ Hz, 2H, OCH$_2$), 2.43 (t, $J = 7.5$ Hz, 2H, COCH$_2$), 2.08 (quint, $J = 7.1$ Hz, 2H, NCH$_2$CH$_2$) and 1.21 ppm (t, $J = 7.1$ Hz, 3H, CH$_3$); ^{13}C NMR (63 MHz, CDCl$_3$): $\delta = 172.8$ (C), 162.3 (C), 152.2 (C), 138.5 (C), 134.9 (CH), 128.1 (CH), 123.2 (CH), 115.1 (CH), 114.4 (C), 60.3 (OCH$_2$), 40.1 (NCH$_2$), 31.7 (CH$_2$), 23.1 (CH$_2$) and 14.0 ppm (CH$_3$); IR (ATR): $\tilde{v} = 2955$ (NH), 1729 (CO) and 1620 cm^{-1} (CO); MS (ESI) m/z: 299 [M+Na]$^+$; HRMS calcd for C$_{14}$H$_{16}$N$_2$O$_4$Na [M+Na]$^+$: 299.1002, found: 299.1013.

3-(2,4-Dioxo-1,4-dihydroquinazolin-3(2H)-yl)propanoic acid (26): A solution of the ester **25** (200 mg, 0.73 mmol) in dry THF (1.5 mL) at room temperature was treated with aqueous LiOH (2.1 mL, 0.7 M). The reaction mixture was stirred at room temperature for 2 h and then washed with diethyl ether. The aqueous phase was acidified with HCl (10%) and extracted with ethyl acetate (×3). The combined organic extracts were dried (anh. Na$_2$SO$_4$), filtered and concentrated under reduced pressure to give the acid **26** (158 mg, 90%) as a white solid; mp: 247–249 °C; ^{1}H NMR (250 MHz, CD$_3$OD): $\delta = 8.03$ (d, $J = 7.9$ Hz, 1H, ArH), 7.64 (t, $J = 7.6$ Hz, 1H, ArH), 7.23 (t, $J = 7.6$ Hz, 1H, ArH), 7.16 (d, $J = 8.2$ Hz, 1H, ArH), 4.09 (t, $J = 6.9$ Hz, 2H, NCH$_2$), 2.39 (t, $J = 7.3$ Hz, 2H, COCH$_2$) and 1.99 ppm (quint, $J = 7.1$ Hz, 2H, NCH$_2$CH$_2$); ^{13}C NMR (63 MHz, CD$_3$OD): $\delta = 176.6$ (C), 164.3 (C), 152.3 (C), 140.7 (C), 136.1 (CH), 128.7 (CH), 123.9 (CH), 116.0 (CH), 115.4 (C), 41.1 (NCH$_2$), 32.3 (CH$_2$) and 24.3 ppm (CH$_2$); IR

(ATR): $\tilde{v} = 3431$ (NH+OH), 1707 (CO), 1688 (CO) and 1650 (CO) cm^{-1}; MS (ESI) m/z: 247 [M−H]$^-$; HRMS calcd for $C_{12}H_{11}N_2O_4$ [M−H]$^-$: 247.0724, found: 247.0721.

Diester 27S: A solution of the acid **26** (80 mg, 0.3 mmol) in thionyl chloride (5 mL) was heated under reflux for 30 min. After cooling to room temperature, the solvent was removed under reduced pressure and the crude residue was dissolved in dry dichloromethane (2 mL) and treated with dry trimethylamine (80 µL, 0.6 mmol) and dimethyl L-aspartate (60 mg, 0.3 mmol). The resulting mixture was stirred at room temperature for 2 h and then washed with saturated NaHCO$_3$ (×3) and brine (×3). The organic extract was dried (anh. Na$_2$SO$_4$), filtered and concentrated under reduced pressure. The resulting residue was purified by flash chromatography, eluting with ethyl acetate, to give the diester **27S** (78 mg, 66%) as a white foam. $\alpha_D^{20} = +27.0°$ ($c = 1.1$, CHCl$_3$); ^{1}H NMR (500 MHz, CDCl$_3$): $\delta = 10.01$ (s, 1H, NH), 8.09 (dd, $J = 0.7$ and $J = 7.9$ Hz, 1H, ArH), 7.60 (td, $J = 1.4$ and $J = 8.2$ Hz, 1H, ArH), 7.21 (t, $J = 7.5$ Hz, 1H, ArH), 7.13 (d, $J = 8.1$ Hz, 1H, ArH), 7.01 (br d, $J = 8.5$ Hz, 1H, NH), 4.89 (dt, $J = 4.6$ and $J = 8.1$ Hz, 1H, CH), 4.16 (m, 2H, NCH$_2$), 3.73 (s, 3H, OCH$_3$), 3.68 (s, 3H, OCH$_3$), 3.02 (dd, $J = 4.7$ and $J = 17.1$ Hz, 1H, CHHCO$_2$Me), 2.87 (dd, $J = 4.6$ and $J = 17.1$ Hz, 1H, CHHCO$_2$Me), 2.36 (m, 2H, CH$_2$CO) and 2.10 ppm (quint, $J = 7.0$ Hz, 2H, CH$_2$CH$_2$CH$_2$); ^{13}C NMR (63 MHz, CDCl$_3$): $\delta = 172.2$ (C), 171.4 (C), 171.2 (C), 162.5 (C), 151.7 (C), 138.6 (C), 134.9 (CH), 128.1 (CH), 123.1 (CH), 115.0 (CH), 114.2 (C), 52.6 (OCH$_3$), 51.9 (OCH$_3$), 48.4 (CH), 40.0 (NCH$_2$), 36.0 (CH$_2$), 33.4 (CH$_2$) and 23.9 ppm (CH$_2$); IR (ATR): $\tilde{v} = 3283$ (NH), 1722 (CO) and 1645 cm^{-1} (CO); MS (ESI): 392 [M+H]$^+$; HRMS calcd for $C_{18}H_{22}N_3O_7$ [M+H]$^+$: 392.1452, found: 392.1452.

Diester 27R: The compound was prepared as its enantiomer **27S** using the acid **26** (60 mg, 0.2 mmol), thionyl chloride (3.5 mL), dry dichloromethane (1.6 mL), dry trimethylamine (67 µL, 0.4 mmol) and dimethyl D-aspartate (48 mg, 0.4 mmol). Yield = 59 mg (63%, white foam). The compound has the same NMR data as its enantiomer **27S**. $\alpha_D^{20} = -25.0°$ ($c = 1.1$, CHCl$_3$); MS (ESI): 392 [M+Na]$^+$; HRMS calcd for $C_{18}H_{21}N_3O_7Na$ [M+Na]$^+$: 414.1272, found: 414.1268.

Diacid 17S: A stirred solution of diester **27S** (30 mg, 0.1 mmol) in THF (1 mL) was treated with LiOH (0.3 mL, 0.6 mmol, 2.5 M). The resulting mixture was stirred at room temperature for 2 h. The reaction mixture was diluted with water and THF was concentrated under reduced pressure. The aqueous solution was washed with ethyl acetate (×3). The aqueous phase was treated with Amberlite IR-120 (H$^+$) until pH 6.0 and filtered. The filtrate and the washings were freeze-dried to afford compound **17S** (22 mg, 79%) as a white solid; mp: 165.3–165.7 °C. $\alpha_D^{20} = +10.2°$ ($c = 0.8$, H$_2$O); ^{1}H NMR (300 MHz, D$_2$O): $\delta = 7.83$ (d, $J = 8.0$ Hz, 1H, ArH), 7.64 (t, $J = 7.2$ Hz, 1H, ArH), 7.23 (t, $J = 7.4$ Hz, 1H, ArH), 7.06 (d, $J = 8.2$ Hz, 1H, ArH), 4.61 (t, $J = 5.9$ Hz, 1H, CH), 3.93 (t, $J = 7.0$ Hz, 2H, NCH$_2$), 2.85 (d, $J = 6.1$ Hz, 2H, CH$_2$CO$_2$H), 2.39 (t, $J = 7.3$ Hz, 2H, CH$_2$CO) and 1.95 ppm (quint, $J = 7.1$ Hz, 2H, CH$_2$CH$_2$CH$_2$); ^{13}C NMR (63 MHz, D$_2$O): $\delta = 177.8$ (C), 177.2 (C), 177.1 (C), 166.6 (C), 154.1 (C), 140.9 (C), 138.2 (CH), 129.6 (CH), 126.1 (CH), 117.6 (CH), 115.9 (C), 52.0 (CH), 42.8 (CH$_2$), 38.5 (CH$_2$), 35.3 (CH$_2$) and 25.5 ppm (CH$_2$); IR (ATR): $\tilde{v} = 3249$ (OH+NH), 1704 (CO), 1644 (CO) and 1622 cm^{-1} (CO); MS (ESI): 362 [M−H]$^-$; HRMS calcd for $C_{16}H_{16}N_3O_7$ [M−H]$^-$: 362.0994, found: 362.0993.

Diacid 17R: The compound was prepared as its enantiomer **17S** using the diester **27R** (70 mg, 0.17 mmol), THF (1.8 mL), and LiOH (0.34 mL, 2.5 M). Yield = 50 mg (79%, white solid). The compound has the same NMR data as its enantiomer **17S**. $\alpha_D^{20} = -10.1°$ ($c = $

0.8, H$_2$O); MS (ESI): 362 [M−H]$^-$; HRMS calcd for $C_{16}H_{16}N_3O_7$ [M−H]$^-$: 362.0994, found: 362.0994.

Acid 30: A solution of 2-((2R,4R)-2-(tert-butyl)-5-oxo-1,3-dioxolan-4-yl)acetic acid (**29**)[43] (300 mg, 1.48 mmol) in dry THF (14.8 mL), under argon and at −78 °C, was treated with LHMDS (2.97 mL, 2.97 mmol, ~1 M in THF). After 30 min, a solution of tert-butyl bromoacetate (0.33 mL, 2.22 mmol) in dry THF (3 mL) was added. The reaction mixture was allowed to warm up to −23 °C and it was stirred at this temperature for another 10 h. HCl (1 M) was added and the reaction mixture was extracted with ethyl acetate (×3). All the organic extracts were dried (anh. Na$_2$SO$_4$), filtered and concentrated under reduced pressure. Purification by flash chromatography, eluting with (91:8:1) dichloromethane/methanol/trimethylamine, gave the ester **30** (164 mg, 35%) as a white solid. $\alpha_D^{20} = +18°$ ($c = 1.7$, CH$_3$OH); ^{1}H NMR (250 MHz, CDCl$_3$): $\delta = 5.30$ (s, 1H, CH), 3.03 (d, $J = 16.1$ Hz, 1H, CHH), 2.95 (d, $J = 15.6$ Hz, 1H, CHH), 2.87 (d, $J = 16.1$ Hz, 1H, CHH), 2.85 (d, $J = 15.6$ Hz, 1H, CHH), 1.16 (s, 9H, C(CH$_3$)$_3$) and 0.96 ppm (s, 9H, C(CH$_3$)$_3$); ^{13}C NMR (63 MHz, CDCl$_3$): $\delta = 174.0$ (C), 173.1 (C), 168.3 (C), 110.0 (CH), 82.5 (C), 77.5 (C), 41.3 (CH$_2$), 40.6 (CH$_2$), 34.6 (C(CH$_3$)$_3$), 28.1 (C(CH$_3$)$_3$) and 23.7 ppm (C(CH$_3$)$_3$); IR (KBr): $\tilde{v} = 3009$ (OH), 1806 (CO), 1724 (CO) and 1708 cm^{-1} (CO); MS (ESI) m/z: 315 [M−H]$^-$; HRMS calcd for $C_{15}H_{23}O_7$ [M−H]$^-$: 315.1449, found: 315.1456.

Amide 31: A stirred solution of acid **30** (16 mg, 0.05 mmol) and amine **24** (24 mg, 0.12 mmol) in dry DMF (3.6 mL), under argon and at room temperature, was treated with HATU (36 mg, 0.09 mmol) and DIPEA (8.5 µL, 0.05 mmol). The resulting mixture was stirred at room temperature for 1 h. The reaction mixture was diluted with ethyl acetate and water. The organic layer was separated and the aqueous phase was extracted with ethyl acetate (×2). The combined organic layers were dried (anh. Na$_2$SO$_4$), filtered and concentrated under reduced pressure. The residue obtained was purified by flash chromatography, eluting with (75:25) ethyl acetate/hexane, to give the amide **31** (15 mg, 60%) as a white solid; mp: 203–205 °C. $\alpha_D^{20} = +6.7°$ ($c = 1.0$, CHCl$_3$); ^{1}H NMR (300 MHz, CDCl$_3$): $\delta = 10.3$ (br s, 1H, NH), 8.05 (dd, $J = 8.0$ and 1.0 Hz, 1H, ArH), 7.68 (m, 1H, ArH), 7.16 (m, 2H, 2×ArH), 6.94 (t, $J = 5.0$ Hz, 1H, NH), 5.26 (s, 1H, CH), 4.27 (t, $J = 5.5$ Hz, 2H, CH$_2$), 3.75–3.55 (m, 2H, CH$_2$), 2.99 (t, $J = 16.6$ Hz, 1H, CHH), 2.99 (d, $J = 16.6$ Hz, 1H, CHH), 2.89 (d, $J = 16.6$ Hz, 1H, CHH), 2.67 (d, $J = 14.7$ Hz, 1H, CHH), 2.60 (d, $J = 14.7$ Hz, 1H, CHH), 1.41 (s, 9H, C(CH$_3$)$_3$) and 0.89 ppm (s, 9H, C(CH$_3$)$_3$); ^{13}C NMR (75 MHz, CDCl$_3$): $\delta = 173.8$ (C), 168.9 (C), 167.8 (C), 163.2 (C), 151.9 (C), 138.9 (C), 135.4 (CH), 128.4 (CH), 123.5 (CH), 115.5 (CH), 114.3 (C), 110.2 (CH), 82.3 (C(CH$_3$)$_3$), 78.0 (C(CH$_3$)$_3$) 44.2 (CH$_2$), 40.9 (CH$_2$), 40.0 (CH$_2$), 39.3 (CH$_2$), 34.5 (C), 28.1 (C(CH$_3$)$_3$) and 23.7 ppm (C(CH$_3$)$_3$); IR (ATR): $\tilde{v} = 3512$ (OH), 3362 (NH), 1793 (CO), 1724 (CO) and 1659 cm^{-1} (CO); MS (ESI) m/z: 526 [M+Na]$^+$; HRMS calcd for $C_{25}H_{33}N_3O_8Na$ [M+Na]$^+$: 526.2160, found: 526.2168.

Ester 32: A stirred solution of ketal **31** (40 mg, 0.08 mmol) in water (0.3 mL) was treated with LiOH (0.7 mL, 0.08 mmol, 0.11 M). The resulting mixture was stirred at room temperature for 4 h. The reaction mixture was diluted with ethyl acetate and water. The organic layer was separated and the aqueous phase was washed with ethyl acetate (×2). The aqueous phase was treated with Amberlite IR-120 (H$^+$) until pH 6.0 and filtered. The filtrate and the washings were freeze-dried to afford compound **32** (30 mg, 88%) as a white solid; mp: 170 °C (dec.). $\alpha_D^{20} = -0.6°$ ($c = 0.9$, CH$_3$CN); ^{1}H NMR (300 MHz, D$_2$O): $\delta = 7.74$ (d, $J = 7.9$ Hz, 1H, ArH), 7.52 (t, $J = 7.8$ Hz, 1H, ArH), 7.11 (t, $J = 7.7$ Hz, 1H, ArH), 6.96 (d, $J = 8.2$ Hz, 1H, ArH), 3.94 (t, $J = 5.7$ Hz, 2H, NCH$_2$), 3.62 (t, $J = 5.7$ Hz, 2H, NCH$_2$), 2.70 (t, $J = 15.4$ Hz, 1H, CHH), 2.51 (d, $J = 14.5$ Hz, 1H, CHH), 2.41 (d, $J = $

15.4 Hz, 1H, CHH), 2.37 (d, $J=14.5$ Hz, 1H, CHH) and 1.25 ppm (s, 9H, C(CH$_3$)$_3$); ^{13}C NMR (63 MHz, D$_2$O): $\delta=172.5$ (C), 171.8 (C), 165.1 (C), 152.5 (C), 139.2 (C), 136.5 (CH), 127.9 (CH), 124.3 (CH), 116.7 (C), 115.9 (CH), 114.1 (C), 83.7 (C), 74.8 (C), 45.6 (CH$_2$), 44.8 (CH$_2$), 40.6 (CH$_2$), 37.7 (CH$_2$) and 27.7 ppm (C(CH$_3$)$_3$); IR (ATR): $\tilde{\nu}=3440$, 3125 and 3355 (OH+NH), 1729, 1710, 1668 and 1652 cm^{-1} (CO); MS (ESI) m/z: 434 $[M-H]^-$; HRMS calcd for C$_{20}$H$_{24}$N$_3$O$_8$ $[M-H]^-$: 434.1569, found: 434.1566.

Acid 18: A stirred solution of ester **32** (10 mg, 0.02 mmol) in water (0.11 mL) was treated with aqueous HCl (0.08 mL, 0.37 mmol, 4.5 M). The resulting mixture was stirred at room temperature for 6 h. The reaction mixture was diluted with ethyl acetate and water. The organic layer was separated and the aqueous phase was washed with ethyl acetate (×2). The aqueous phase was freeze-dried to afford the acid **18** (7 mg, 78%) as a white solid; mp: 151–152 °C. $\alpha_D^{20}=+1.6°$ ($c=0.8$, H$_2$O); ^{1}H NMR (500 MHz, D$_2$O): $\delta=7.83$ (d, $J=8.0$ Hz, 1H, ArH), 7.56 (t, $J=7.7$ Hz, 1H, ArH), 7.15 (t, $J=7.7$ Hz, 1H, ArH), 7.05 (d, $J=8.3$ Hz, 1H, ArH), 3.99 (m, 2H, NCH$_2$), 3.44–3.32 (m, 2H, NCH$_2$), 2.77 (t, $J=16.1$ Hz, 1H, CHH), 2.52 (d, $J=15.3$ Hz, 2H, CHH+CHH) and 1.25 ppm (d, $J=14.6$ Hz, 1H, CHH); ^{13}C NMR (100 MHz, D$_2$O): $\delta=176.4$ (C), 173.3 (C), 171.1 (C), 164.3 (C), 151.7 (C), 138.4 (C), 135.7 (CH), 127.1 (CH), 123.6 (CH), 115.1 (CH), 113.3 (C), 73.3 (C), 44.4 (CH$_2$), 42.6 (CH$_2$), 39.9 (CH$_2$) and 36.9 ppm (CH$_2$); IR (ATR): $\tilde{\nu}=3264$, 3095, 2917 and 2850 (OH+NH), 1704, 1644 and 1622 cm^{-1} (CO); MS (ESI) m/z: 378 $[M-H]^-$; HRMS calcd for C$_{16}$H$_{16}$N$_3$O$_8$ $[M-H]^-$: 378.0943, found: 378.0942.

3-Allylquinazoline-2,4(1H,3H)-dione (33): A suspension of N-allyl-2-aminobenzamide (50 mg, 0.26 mmol), which was prepared as indicated below, in dry dichloromethane (1.3 mL), under inert atmosphere and at room temperature, was treated with triphosgene (38 mg, 0.13 mmol) and DIPEA (0.1 mL, 0.052 mmol). The resulting solution was stirred for 1 h and then diluted with dichloromethane and saturated solution of NaHCO$_3$. The aqueous phase was separated and the organic layer was washed with water. The organic extract was dried (anh. Na$_2$SO$_4$), filtered and concentrated under reduced pressure. The residue obtained was purified by flash chromatography, eluting with (75:25) ethyl acetate/hexane, to give the quinazolinedione **33** (35 mg, 61%) as a yellow solid; mp: 221–224 °C; ^{1}H NMR (300 MHz, CDCl$_3$): $\delta=10.82$ (br s, 1H, NH), 8.26 (d, $J=7.9$ Hz, 1H, ArH), 7.61 (t, $J=8.1$ Hz, 1H, ArH), 7.23 (d, $J=7.9$ Hz, 1H, ArH), 7.17 (t, $J=8.1$ Hz, 1H, ArH), 5.95–5.82 (m, 1H CH=CH$_2$), 5.12–5.01 (m, 2H, CH=CH$_2$), 4.19 (t, $J=7.1$ Hz, 2H, CH$_2$) and 2.51 ppm (q, $J=7.1$ Hz, 2H, CH$_2$); ^{13}C NMR (63 MHz, CDCl$_3$): $\delta=162.3$ (C), 152.4 (C), 138.7 (C), 134.9 (C), 134.8 (CH), 128.3 (C), 123.3 (C), 117.1 (C), 115.1 (C), 114.6 (CH$_2$), 40.2 (CH$_2$) and 32.9 ppm (CH$_2$); IR (ATR): $\tilde{\nu}=3183$ (NH), 1714 (CO) and 1629 cm^{-1} (CO); MS (ESI) m/z: 217 $[M+H]^+$; HRMS calcd for C$_{12}$H$_{13}$N$_2$O$_2$ $[M+H]^+$: 217.0972, found: 217.0969.

N-Allyl-2-aminobenzamide: An stirred solution of anthranilic acid (**30**) (100 mg, 0.73 mmol) in dry DMF (3.6 mL), under argon and at room temperature, was treated with EDC (168 mg, 0.87 mmol), N,N-dimethylpyridine (4.8 mg, 0.04 mmol), DIPEA (0.25 mL, 0.15 mmol) and 3-butenylamine (120 mg, 0.11 mmol). The resulting mixture was stirred at room temperature for 1 h. The reaction mixture was diluted with ethyl acetate and water. The organic layer was separated and the aqueous phase was extracted with ethyl acetate (×2). The combined organic layers were dried (anh. Na$_2$SO$_4$), filtered and concentrated under reduced pressure. The residue obtained was purified by flash chromatography, eluting with (20:800) ethyl acetate/hexane, to give N-allyl-2-aminobenzamide (105 mg, 70%) as a white solid; mp: 181–184 °C; ^{1}H NMR (300 MHz, CDCl$_3$): $\delta=7.28$–7.25 (d, $J=7.8$ Hz, 1H, ArH), 7.19–7.13 (t,

$J=7.7$ Hz, 1H, ArH) 6.64 (d, $J=8.8$ Hz, 1H, ArH), 6.59 (t, $J=8.2$ Hz, 1H, ArH), 6.27 (br s, 1H, NH), 5.86–5.72 (m, 1H, CH=CH$_2$), 5.48 (br s, 2H, NH$_2$), 5.15–5.07 (m, 2H, HC=CH$_2$), 3.44 (q, $J=6.4$ Hz, 2H, CH$_2$) and 2.32 ppm (q, $J=6.7$ Hz, 2H, CH$_2$); ^{13}C NMR (63 MHz, CDCl$_3$): $\delta=169.2$ (C), 148.6 (C), 135.3 (C), 132.1 (CH), 127.1 (CH), 117.3 (CH), 117.2 (CH), 116.6 (CH$_2$), 116.3 (C), 38.5 (CH) and 33.7 ppm (CH$_2$); IR (ATR): $\tilde{\nu}=3295$ (NH) and 1616 cm^{-1} (CO); MS (ESI) m/z: 191 $[M+H]^+$; HRMS calcd for C$_{11}$H$_{15}$N$_2$O $[M+H]^+$: 191.1179, found: 191.1178.

Methyl (2S,4S)-2-[(E)-4-(5-bromo-2-pentenyl)-2-(tert-butyl)-5-oxo-1,3-dioxolan-4-yl)]acetate (36): A solution of alkene **34**[43] (160 mg, 0.62 mmol) and 4-bromobutene (63 µL, 0.62 mmol) in dry toluene (3 mL) under inert atmosphere was treated with second generation Grubbs–Hoveyda catalyst (78 µg, 0.12 mmol) and heated at 90 °C for 16 h. After cooling to room temperature, the reaction mixture was filtered through Celite. The filtrate and the washings were concentrated under reduced pressure and the resulting brown oil was purified by flash chromatography, eluting with (50:50) diethyl ether/hexane, to yield the bromide **36** (185 mg, 77%) as a yellow oil. $\alpha_D^{20}=+2.2°$ ($c=1.0$, CHCl$_3$); ^{1}H NMR (250 MHz, CDCl$_3$): $\delta=5.62$–5.50 (m, 2H, CH=CH), 5.19 (s, 1H, CH), 3.63 (s, 3H, OCH$_3$), 3.37 (t, $J=6.6$ Hz, 2H, BrCH$_2$), 2.78 (s, 2H, CH$_2$CO$_2$), 2.61–2.48 (m, 4H, CH$_2$CH=CHCH$_2$), and 0.90 ppm (s, 9H, 3×CH$_3$); ^{13}C NMR (63 MHz, CD$_3$OD): $\delta=173.5$ (C), 168.6 (C), 133.2 (CH), 124.8 (CH), 108.1 (CH), 79.9 (C), 51.9 (OCH$_3$), 39.7 (CH$_2$), 37.0 (CH$_2$), 35.5 (CH$_2$), 34.1 (C(CH$_3$)$_3$), 32.1 (CH$_2$) and 23.4 ppm (3×CH$_3$); IR (ATR): $\tilde{\nu}=1795$ (CO) and 1743 cm^{-1} (CO); MS (ESI) m/z: 385 and 387 $[M+Na]^+$; HRMS calcd for C$_{15}$H$_{23}$Br^{79}O$_5$Na $[M+Na]^+$: 385.0621, found: 385.0621.

Methyl (2S,4S)-4-[(E)-4-(5-azido-2-pentenyl)]-2-(tert-butyl)-5-oxo-1,3-dioxolan-4-yl)acetate (37): A solution of bromide **36** (60 mg, 0.15 mmol), sodium azide (40 mg, 0.62 mmol) in dry DMF (4 mL) under inert atmosphere was heated at 90 °C for 2 h. After cooling to room temperature, the reaction mixture was diluted with ethyl acetate and water (1:4). The organic layer was separated and the aqueous layer was extracted with ethyl acetate (×3). The combined organic extracts were washed with water, dried (anh. Na$_2$SO$_4$), filtered and concentrated under reduced pressure. The resulting residue was purified by flash chromatography, eluting with (50:50) diethyl ether/hexane, to afford the azide **37** (39 mg, 74%) as a colorless oil. $\alpha_D^{20}=+10.4°$ ($c=1.0$, CHCl$_3$); ^{1}H NMR (250 MHz, CDCl$_3$): $\delta=5.58$–5.51 (m, 2H, HC=CH), 5.18 (s, 1H, CH), 3.63 (s, 3H, OCH$_3$), 3.29 (t, $J=6.6$ Hz, 2H, N$_3$CH$_2$), 2.77 (s, 2H, CH$_2$CO$_2$), 2.50–2.48 (m, 2H, CH$_2$CH), 2.34–2.27 (q, $J=6.2$ Hz, 2H, CHCH$_2$) and 0.91 ppm (s, 9H, 3×CH$_3$); ^{13}C NMR (63 MHz, CDCl$_3$): $\delta=173.4$ (C), 168.6 (C), 132.4 (CH), 124.8 (CH), 108.2 (CH), 79.9 (C), 51.9 (OCH$_3$), 50.5 (CH$_2$), 39.6 (CH$_2$), 37.0 (CH$_2$), 34.1 (C(CH$_3$)$_3$), 32.0 (CH$_2$) and 23.4 ppm (3×CH$_3$); IR (ATR): $\tilde{\nu}=2095$ (N$_3$), 1798 and 1746 cm^{-1} (CO); MS (ESI) m/z: 348 $[M+Na]^+$; HRMS calcd for C$_{15}$H$_{23}$N$_3$O$_5$Na $[M+Na]^+$: 348.1530, found: 348.1530.

Methyl (2S,4S)-4-[(E)-5-(2-aminobenzamido-2-pentenyl]-2-(tert-butyl)-5-oxo-1,3-dioxolan-4-ylacetate (38): A solution of azide **37** (170 mg, 0.6 mmol) in tetrahydrofuran (15 mL) was treated with triphenylphosphine (180 mg, 0.6 mmol) and distilled water (0.15 mL) and heated under reflux for 12 h. After cooling to room temperature, the solvent was removed under reduced pressure. The resulting crude mixture was dissolved under inert atmosphere in dry dichloromethane (2.5 mL) and then treated with EDC (340 mg, 1.7 mmol), DMAP (53 mg, 0.4 mmol) and anthranilic acid (**20**) (130 mg, 0.4 mmol). The resulting mixture was stirred at room temperature for 1 h and then diluted with dichloromethane and saturated sodium bicarbonate. The aqueous layers were extracted with dichloromethane (×3). The combined organic extracts were

washed with water, dried (anh. Na$_2$SO$_4$), filtered and concentrated under reduced pressure. The resulting residue was purified by flash chromatography, eluting with (4:1) diethyl ether/ethyl acetate, to give the amide **38** (105 mg, 74%) as a white foam. $\alpha_D^{20} = -5.8°$ ($c =$ 1.0, CHCl$_3$); ^{1}H NMR (250 MHz, CDCl$_3$): $\delta = 7.35$ (d, $J = 8.0$ Hz, 1 H, ArH), 7.17 (t, $J = 7.7$ Hz, 1 H, ArH), 6.67 (d, $J = 8.1$ Hz, 1 H, ArH), 6.60 (t, $J = 7.3$ Hz, 1 H, ArH), 6.44 (br s, 1 H, NH), 5.66–5.40 (m, 3 H, NH + CH=CH), 5.18 (s, 1 H, CH), 3.63 (s, 3 H, OCH$_3$), 3.57–3.30 (m, 2 H, NHCH$_2$), 2.73 (s, 2 H, CH$_2$CO$_2$), 2.50 (d, $J = 6.8$ Hz, 2 H, NCH$_2$CH_2) 2.32 (q, $J = 6.6$ Hz, 2 H, HC=CHCH_2), and 0.92 ppm (s, 9 H, 3×CH$_3$); ^{13}C NMR (63 MHz, CDCl$_3$): $\delta = 173.2$ (C), 169.2 (C), 168.5 (C), 148.2 (C), 133.8 (CH), 132.0 (CH), 127.1 (CH), 124.0 (CH), 117.2 (CH), 116.7 (CH), 116.0 (C), 107.9 (CH), 80.0 (C), 51.9 (OCH$_3$), 39.2 (CH$_2$), 38.5 (CH$_2$), 36.6 (CH$_2$), 34.1 (*C*(CH$_3$)$_3$), 32.6 (CH$_2$) and 23.4 ppm (3×CH$_3$); IR (ATR): $\tilde{\nu} = 3168$ (NH), 3096 (NH), 1773 (CO) and 1738 cm^{-1} (CO); MS (ESI) m/z: 419 $[M+H]^+$; HRMS calcd for C$_{22}$H$_{31}$N$_2$O$_6$ $[M+H]^+$: 419.2177, found: 419.2180.

Quinazolinedione 39: A solution of the aniline **38** (40 mg, 0.1 mmol) and triethylamine (27 μL, 0.2 mmol) in dry dichloromethane (0.5 mL), under inert atmosphere and at room temperature, was treated with a solution of triphosgene (18 mg, 0.06 mmol) in dry dichloromethane (0.3 mL). The reaction mixture was stirred at room temperature for 2 h and then washed with HCl (10%, ×3). The combined aqueous layers were extracted with dichloromethane (×3). The combined organic extracts were washed with water, dried (anh. Na$_2$SO$_4$), filtered and concentrated under reduced pressure. The resulting residue was purified by flash chromatography, eluting with (4:1) diethyl ether/ethyl acetate, to afford the quinazolinedione **39** (31 mg, 70%) as a white foam. $\alpha_D^{20} = +5.7°$ ($c = 1.25$, CHCl$_3$); ^{1}H NMR (300 MHz, CDCl$_3$): $\delta = 9.85$ (br s, 1 H, NH), 8.11 (d, $J = 7.9$ Hz, 1 H, ArH), 7.60 (td, $J = 1.5$ and 7.4 Hz, 1 H, ArH), 7.22 (td, $J = 0.9$ and 8.0 Hz, 1 H, ArH), 7.10 (d, $J = 8.0$ Hz, 1 H, ArH), 5.71 (m, 1 H, CH=CH), 5.44 (m, 1 H, CH=CH), 5.11 (s, 1 H, CH), 4.15 (t, $J = 7.0$ Hz, 2 H, NCH$_2$), 3.63 (s, 3 H, OCH$_3$), 2.76 (s, 2 H, CH$_2$CO$_2$), 2.50–2.41 (m, 4 H, CH_2CH=CHCH_2) and 0.87 ppm (s, 9 H, 3×CH$_3$); ^{13}C NMR (63 MHz, CDCl$_3$): $\delta = 173.5$ (C), 168.8 (C), 162.2 (C), 151.8 (C), 138.5 (C), 134.9 (C), 133.0 (CH), 128.2 (CH), 124.0 (CH), 123.2 (CH), 115.0 (CH), 114.3 (C), 107.9 (CH), 79.9 (C), 51.8 (OCH$_3$), 39.9 (CH$_2$), 39.3 (CH$_2$), 36.7 (CH$_2$), 34.0 (*C*(CH$_3$)$_3$), 31.1 (CH$_2$) and 23.4 ppm (3×CH$_3$); IR (ATR): $\tilde{\nu} = 2952$ (NH), 1795 (CO), 1748 (CO), 1717 (CO) and 1659 cm^{-1} (CO); MS (ESI) m/z: 445 $[M+H]^+$; HRMS calcd for C$_{23}$H$_{29}$N$_2$O$_7$ $[M+H]^+$: 445.1969, found: 445.1975.

Quinazolinedione 40: A solution of the alkene **39** (45 mg, 0.1 mmol) in ethanol (1 mL) under hydrogen atmosphere was added via cannula to a suspension of Pd-C (5 mg, 10%) in ethanol (0.5 mL) under hydrogen atmosphere. The resulting suspension was stirred at room temperature for 12 h. Hydrogen was removed under vacuo and the suspension was filtered through a plug of Celite. The filtrate and the washings were concentrated under reduced pressure. The resulting residue was purified by flash chromatography, eluting with (4:1) diethyl ether/ethyl acetate, to afford the saturated quinazolinedione **40** (38 mg, 84%) as a white foam. $\alpha_D^{20} = +7.3°$ ($c = 1.25$, CHCl$_3$); ^{1}H NMR (250 MHz, CDCl$_3$): $\delta = 10.20$ (s, 1 H, NH), 8.12 (dd, $J = 8.0$ and 1.0 Hz, 1 H, ArH), 7.63 (td, $J = 8.5$ and 1.4 Hz, 1 H, ArH), 7.24 (t, $J = 7.9$ Hz, 1 H, ArH), 7.13 (d, $J = 8.1$ Hz, 1 H, ArH), 5.16 (s, 1 H, CH), 4.08 (t, $J = 7.2$ Hz, 2 H, NCH$_2$), 3.66 (s, 3 H, OCH$_3$), 2.82 (s, 2 H, CH$_2$CO$_2$), 1.86–1.71 (m, 4 H, 2×CH$_2$) and 0.93 ppm (s, 9 H, 3×CH$_3$); ^{13}C NMR (63 MHz, CD$_3$OD): $\delta = 173.6$ (C), 168.5 (C), 162.0 (C), 151.6 (C), 138.1 (C), 134.7 (CH), 128.0 (CH), 123.1 (CH), 114.6 (CH), 114.2 (C), 107.8 (CH), 79.8 (C), 51.6 (OCH$_3$), 40.3 (CH$_2$), 39.2 (CH$_2$), 33.9 (CH$_2$), 33.2 (*C*(CH$_3$)$_3$), 27.2 (CH$_2$), 26.5 (CH$_2$), 23.2 (3×CH$_3$) and 22.6 ppm (CH$_2$); IR (ATR): $\tilde{\nu} = 2952$ (NH),

1790 (CO), 1743 (CO), 1711 (CO) and 1649 cm^{-1} (CO); MS (ESI) m/z: 447 $[M+H]^+$; HRMS calcd for C$_{22}$H$_{31}$N$_2$O$_7$ $[M+H]^+$: 447.2126, found: 447.2120.

Acid 19: A solution of the diester **40** (35 mg, 0.08 mmol) in THF (0.8 mL) was treated with aqueous LiOH (4.8 mL, 0.48 mmol, 0.1 M) and stirred at room temperature for 6 h. The reaction mixture was diluted with ethyl acetate and Milli-Q water. The organic layer was separated and the aqueous extract was washed with ethyl acetate (×3). The aqueous layer was treated with Amberlite IR-120 (H$^+$) until pH 6. The filtrate and the washings were lyophilized to give the acid **19** (22 mg, 76%) as a white solid. $\alpha_D^{20} = -14.0°$ ($c = 1.0$, H$_2$O); mp: 177.9–178.1 °C; ^{1}H NMR (500 MHz, D$_2$O): $\delta = 8.10$ (d, $J = 8.0$ Hz, 1 H, ArH), 7.83 (td, $J = 7.9$ Hz and 1.3 Hz, 1 H, ArH), 7.42 (t, $J = 7.7$ Hz, 1 H, ArH), 7.31 (t, $J = 8.2$, 1 H, ArH), 4.07 (t, $J = 7.3$ Hz, 2 H, NCH$_2$), 3.15 (d, $J = 16.3$ Hz, 1 H, CHH), 2.86 (d, $J = 16.3$ Hz, 1 H, CHH), 1.94–1.81 (m, 2 H, CH$_2$), 1.75 (q, $J = 7.7$ Hz, 2 H, CH$_2$), 1.68–1.56 (m, 1 H, CHH), 1.48 (q, $J = 7.6$ Hz, 2 H, CH$_2$) and 1.44–1.37 ppm (m, 1 H, CHH); ^{13}C NMR (63 MHz, D$_2$O): $\delta = 178.4$ (C), 174.5 (C), 164.6 (C), 152.1 (C), 138.8 (C), 136.0 (CH), 127.5 (CH), 123.9 (CH), 115.5 (CH), 113.9 (C), 75.8 (C), 43.5 (CH$_2$), 41.2 (CH$_2$), 38.8 (CH$_2$), 26.9 (CH$_2$), 26.3 (CH$_2$) and 22.5 ppm (CH$_2$); IR (ATR): $\tilde{\nu} = 3325$ (OH) and 1582 cm^{-1} (CO); MS (ESI) m/z: 363 $[M-H]^-$; HRMS calcd for C$_{17}$H$_{19}$N$_2$O$_7$ $[M-H]^-$: 363.1198, found: 363.1198.

Acknowledgements

Conflict of interest

The authors declare no conflict of interest.

[1] a) E. D. Brown, G. D. Wright, *Nature* **2016**, *529*, 336–343; b) M. A. Fischbach, C. T. Walsh, *Science* **2009**, *325*, 1089–1093; c) D. Brown, *Nat. Rev. Drug Discovery* **2015**, *14*, 821–832; d) M. F. Chellat, L. Raguž, R. Reidl, *Angew. Chem. Int. Ed.* **2016**, *55*, 6600–6626; *Angew. Chem.* **2016**, *128*, 6710–6738; e) R. J. Fair, Y. Tor, *Perspect. Med. Chem.* **2014**, *6*, 25–64.

[2] "Enzymology and Molecular Biology of the Shikimate Pathway": C. Abell in *Comprehensive Natural Products Chemistry, Vol. 1* (Ed.: U. Sankawa), Elsevier, Oxford, **1999**, pp. 573–607.

[3] For a database of essential bacterial genes, see http://www.essentialgene.org (accessed August 30, 2017).

[4] G. Lamichhane, J. S. Freundlich, S. Ekins, N. Wickramaratne, S. T. Nolan, W. R. Bisha, *mBio* **2011**, *2*, e00301-10.

[5] C. Coderch, E. Lence, A. Peón, H. Lamb, A. R. Hawkins, F. Gago, C. González-Bello, *Biochem. J.* **2014**, *458*, 547–557.

[6] J. M. Harris, C. Gonzalez-Bello, C. Kleanthous, A. R. Hawkins, J. R. Coggins, C. Abell, *Biochem. J.* **1996**, *319*, 333–336.

[7] C. González-Bello, *Curr. Top. Med. Chem.* **2016**, *16*, 960–977.

[8] a) E. Z. Eisenmesser, M. Akke, D. A. Bosco, D. Kern, *Science* **2002**, *295*, 1520–1523; b) S. J. Benkovic, S. Hammes-Schiffer, *Science* **2003**, *301*, 1196–1202; c) M. Garcia-Viloca, J. Gao, M. Karplus, D. G. Truhlar, *Science* **2004**, *303*, 186–195; d) E. Z. Eisenmesser, O. Millet, V. Labeikovsky, D. M. Korzhnev, M. Wolf-Watz, D. A. Bosco, J. J. Skalicky, L. E. Kay, D. Kern, *Nature* **2005**, *438*, 117–121; e) R. Callender, R. B. Dyer, *Acc. Chem. Res.* **2015**, *48*, 407–413; f) P. Hanoian, C. T. Liu, S. Hammes-Schiffer, S. Benkovic, *Acc. Chem. Res.* **2015**, *48*, 482–489.

[9] For enolate intermediate mimetics, see: a) M. Frederickson, E. J. Parker, A. R. Hawkins, J. R. Coggins, C. Abell, *J. Org. Chem.* **1999**, *64*, 2612–2613; b) M. Frederickson, J. R. Coggins, C. Abell, *Chem. Commun.* **2002**, 1886–1887; c) C. González-Bello, E. Lence, M. D. Toscano, L. Castedo, J. R. Coggins, C. Abell, *J. Med. Chem.* **2003**, *46*, 5735–5744; d) M. Frederickson, A. W. Roszak, J. R. Coggins, A. J. Lapthorn, C. Abell, *Org. Biomol. Chem.* **2004**, *2*, 1592–1596; e) C. Sánchez-Sixto, V. F. V. Prazeres, L. Castedo, H. Lamb, A. R. Hawkins, C. González-Bello, *J. Med. Chem.* **2005**, *48*, 4871–4881; f) V. F. V. Prazeres, C. Sánchez-Sixto, L. Castedo, A. Canales, F. J. Cañada, J. Jiménez-Barbero, H. Lamb, A. R. Hawkins, C. González-Bello, *ChemMedChem* **2006**, *1*, 990–996; g) V. F. V. Prazeres, C. Sánchez-Sixto, L. Castedo, H. Lamb, A. R. Hawkins, A. Riboldi-Tunnicliffe, J. R. Coggins, A. J. Lapthorn, C. González-Bello, *ChemMedChem* **2007**, *2*, 194–207; h) M. D. Toscano, R. J. Payne, A. Chiba, O. Kerbarh, C. Abell, *ChemMedChem* **2007**, *2*, 101–112; i) R. J. Payne, A. Riboldi-Tunnicliffe, O. Kerbarh, A. D. Abell, A. J. Lapthorn, C. Abell, *ChemMedChem* **2007**, *2*, 1010–1013; j) R. J. Payne, F. Peyrot, O. Kerbarh, A. D. Abell, C. Abell, *ChemMedChem* **2007**, *2*, 1015–1029; k) C. Sánchez-Sixto, V. F. V. Prazeres, L. Castedo, S. W. Shuh, H. Lamb, A. R. Hawkins, F. J. Cañada, J. Jiménez-Barbero, C. González-Bello, *ChemMedChem* **2008**, *3*, 756–770; l) A. T. Tran, K. M. Cergol, W. J. Britton, S. A. I. Bokhari, M. Ibrahim, A. J. Lapthorn, R. J. Payne, *MedChemComm* **2010**, *1*, 271–275; m) V. F. V. Prazeres, L. Tizón, J. M. Otero, P. Guardado-Calvo, A. L. Llamas-Saiz, M. J. van Raaij, L. Castedo, H. Lamb, A. R. Hawkins, C. González-Bello, *J. Med. Chem.* **2010**, *53*, 191–200; n) A. T. Tran, K. M. Cergol, N. P. West, E. J. Randall, W. J. Britton, S. A. Bokhari, M. Ibrahim, A. J. Lapthorn, R. J. Payne, *ChemMedChem* **2011**, *6*, 262–265; o) S. Paz, L. Tizón, J. M. Otero, A. L. Llamas-Saiz, G. C. Fox, M. J. van Raaij, H. Lamb, A. R. Hawkins, A. J. Lapthorn, L. Castedo, C. González-Bello, *ChemMedChem* **2011**, *6*, 266–272; p) L. Tizón, J. M. Otero, V. F. V. Prazeres, A. L. Llamas-Saiz, G. C. Fox, M. J. van Raaij, H. Lamb, A. R. Hawkins, J. A. Ainsa, L. Castedo, C. González-Bello, *J. Med. Chem.* **2011**, *54*, 6063–6084; q) B. Blanco, A. Sedes, A. Peón, H. Lamb, A. R. Hawkins, L. Castedo, C. González-Bello, *Org. Biomol. Chem.* **2012**, *10*, 3662–3676; r) B. Blanco, A. Sedes, A. Peón, J. M. Otero, M. J. van Raaij, P. Thompson, A. R. Hawkins, C. González-Bello, *J. Med. Chem.* **2014**, *57*, 3494–3510.

[10] For substrate mimetics, see: a) V. F. V. Prazeres, L. Castedo, H. Lamb, A. R. Hawkins, C. González-Bello, *ChemMedChem* **2009**, *4*, 1980–1984; b) A. Peón, J. M. Otero, L. Tizón, V. F. V. Prazeres, A. L. Llamas-Saiz, G. C. Fox, M. J. van Raaij, H. Lamb, A. R. Hawkins, F. Gago, L. Castedo, C. González-Bello, *ChemMedChem* **2010**, *5*, 1726–1733; c) L. Lence, L. Tizón, J. M. Otero, A. Peón, V. F. V. Prazeres, A. L. Llamas-Saiz, G. C. Fox, M. J. van Raaij, H. Lamb, A. R. Hawkins, C. González-Bello, *ACS Chem. Biol.* **2013**, *8*, 568–577.

[11] N. I. Howard, M. V. B. Dias, F. Peryot, L. Chen, M. F. Schmidt, T. L. Blundell, C. Abell, *ChemMedChem* **2015**, *10*, 116–133.

[12] For examples of crystal structures of the DHQ2 enzyme with an inappropriate arrangement of the substrate-covering loop caused by inhibitor binding, see: a) For *M. tuberculosis* DHQ2: PDB IDs 2XB8,[10b] 2Y71,[9p] and 4B6Q;[10c] b) For *H. pylori* DHQ2: PDB IDs 2WKS,[10m] 2XB9,[10b] and 4B6S.[10c]

[13] N. C. Price, D. J. Boam, S. M. Kelly, D. Duncan, T. Krell, D. G. Gourley, J. R. Coggins, V. Virden, A. R. Hawkins, *Biochem. J.* **1999**, *338*, 195–202.

[14] A. Peón, C. Coderch, F. Gago, C. González-Bello, *ChemMedChem* **2013**, *8*, 740–747.

[15] M. V. Dias, W. C. Snee, K. M. Bromfield, R. J. Payne, S. K. Palaninathan, A. Ciulli, N. I. Howard, C. Abell, J. C. Sacchettini, T. L. Blundell, *Biochem. J.* **2011**, *436*, 729–739.

[16] C. W. Murray, D. C. Rees, *Nat. Chem.* **2009**, *1*, 187–192.

[17] R. A. E. Carr, M. Congreve, C. W. Murray, D. C. Rees, *Drug Discovery Today* **2005**, *10*, 987–992.

[18] D. C. Rees, M. Congreve, C. W. Murray, R. Carr, *Nat. Rev. Drug Discovery* **2004**, *3*, 660–672.

[19] H. L. Silvestre, T. L. Blundell, C. Abell, A. Ciulli, *Proc. Natl. Acad. Sci. USA* **2013**, *110*, 12984–12989.

[20] D. A. Erlanson, R. S. McDowell, T. O'Brien, *J. Med. Chem.* **2004**, *47*, 3463–3482.

[21] D. E. Scott, A. G. Coyne, S. A. Hudson, C. Abell, *Biochemistry* **2012**, *51*, 4990–5003.

[22] *Fragment-Based Drug Discovery: A Practical Approach* (Eds.: E. R. Zartler, M. J. Shapiro), Wiley, Chichester, **2008**.

[23] D. Huang, A. Caflisch, *Fragment-Based Approaches in Virtual Screening: Principles, Challenges, and Practical Guidelines* (Ed.: C. Sotriffer), Wiley-VCH, Weinheim, **2011**.

[24] M. Congreve, G. Chessari, D. Tisi, A. J. Woodhead, *J. Med. Chem.* **2008**, *51*, 3661–3680.

[25] D. Fattori, *Drug Discovery Today* **2004**, *9*, 229–238.

[26] M. Congreve, C. W. Murray, T. L. Blundell, *Drug Discovery Today* **2005**, *10*, 895–907.

[27] D. Huang, A. Caflisch, *J. Mol. Recognit.* **2010**, *23*, 183–193.

[28] P. Kolb, C. B. Kipouros, D. Huang, A. Caflisch, *Proteins Struct. Funct. Bioinf.* **2008**, *73*, 11–18.

[29] K. Lafleur, J. Dong, D. Huang, A. Caflisch, C. Nevado, *J. Med. Chem.* **2013**, *56*, 84–96.

[30] D. Ekonomiuk, X.-C. Su, C. Bodenreider, S. P. Lim, G. Otting, D. Huang, A. Caflisch, *J. Med. Chem.* **2009**, *52*, 4860–4868.

[31] P. Schenker, P. Alfarano, P. Kolb, A. Caflisch, A. Baici, *Protein Sci.* **2008**, *17*, 2145–2155.

[32] P. Kolb, D. Huang, F. Dey, A. Caflisch, *J. Med. Chem.* **2008**, *51*, 1179–1188.

[33] D. Spiliotopoulos, A. Caflisch, *Drug Discovery Today: Technol.* **2016**, *19*, 81–90.

[34] ZINC Database, Univeristy of California, San Francisco: http://zinc.docking.org (accessed August 30, 2017).

[35] P. Kolb, A. Caflisch, *J. Med. Chem.* **2006**, *49*, 7384–7392.

[36] N. Majeux, M. Scarsi, A. Caflisch, *Proteins Struct. Funct. Bioinf.* **2001**, *42*, 256–268.

[37] N. Budin, N. Majeux, A. Caflisch, *Biol. Chem.* **2001**, *382*, 1365–1372.

[38] B. R. Brooks, C. L. Brooks III, A. D. J. Mackerell, L. Nilsson, R. J. Petrella, B. Roux, Y. Won, G. Archontis, C. Bartels, S. Boresch, A. Caflisch, L. Caves, Q. Cui, A. R. Dinner, M. Feig, S. Fischer, J. Gao, M. Hodoscek, W. Im, K. Kuczera, T. Lazaridis, J. Ma, V. Ovchinnikov, E. Paci, R. W. Pastor, C. B. Post, J. Z. Pu, M. S. Schaefer, B. Tidor, R. M. Venable, H. L. Woodcock, X. Wu, W. Yang, D. M. York, M. Karplus, *J. Comput. Chem.* **2009**, *30*, 1545–1614.

[39] D. Huang, A. Caflisch, *J. Med. Chem.* **2004**, *47*, 5791–5797.

[40] L. D. B. Evans, A. W. Roszak, L. J. Noble, D. A. Robinson, P. A. Chalk, J. L. Matthews, J. R. Coggins, N. C. Price, A. J. Lapthorn, *FEBS Lett.* **2002**, *530*, 24–30.

[41] D. A. Robinson, K. A. Stewart, N. C. Price, P. A. Chalk, J. R. Coggins, A. J. Lapthorn, *J. Med. Chem.* **2006**, *49*, 1282–1290.

[42] D. Seebach, A. R. Sting, M. Hoffmann, *Angew. Chem. Int. Ed. Engl.* **1996**, *35*, 2708–2748; *Angew. Chem.* **1996**, *108*, 2881–2921.

[43] T.-H. N. Nguyen, T.-T. T. Bui, P. V. Pham, D. H. Mac, *Tetrahedron Lett.* **2016**, *57*, 216–218.

[44] A. K. Chatterjee, T.-L. Choi, D. P. Sanders, R. H. Grubbs, *J. Am. Chem. Soc.* **2003**, *125*, 11360–11370.

[45] Gold, v.5.2, The Cambridge Crystallographic Data Centre: https://www.ccdc.cam.ac.uk/solutions/csd-discovery/components/gold/ (accessed August 30, 2017).